# UNIVERSITY OF NAIROBI

## School of Engineering

### Department of Environmental and Biosystems Engineering

**Numerical Simulation of Soil Resistance in Ripping: A case study of a Sandy Clay Soil**


By

**Ndisya John Mulwa**

**B.Sc. Env. & Bio. Eng. (2012)**


A Thesis submitted in partial fulfillment for the Degree of Master of Science in Environmental and Biosystems Engineering, in the Department of Environmental and Biosystems Engineering of the University of Nairobi

**October 2015**

## Declaration of originality

| | |
|---|---|
| **Name of student:** | John Mulwa Ndisya |
| **Registration:** | F56/69345/2013 |
| **College:** | Architecture and Engineering |
| **Faculty/School/Institute:** | Engineering |
| **Department:** | Environmental and Biosystems Engineering |
| **Course Name:** | M.Sc in Environmental and Biosystems Engineering |
| **Title of work:** | Numerical simulation of soil resistance in ripping: A case study of a sandy clay soil |

1) I understand what plagiarism is and I'm aware of the university policy in this regard
2) I declare that this research proposal is my original work and has not been submitted elsewhere for examination, award of a degree or publication. Where other works or my own work has been used, this has properly been acknowledged and referenced in accordance with the University of Nairobi's requirements
3) I have not sought or used the services of any professional agencies to produce this work
4) I have not allowed , and shall not allow anyone to copy my work with the intention of passing it off as his/her work
5) I understand that any false claim in respect of this work shall result in disciplinary action in accordance with University of Nairobi anti-plagiarism policy

Signature: _____

Date: _____

## Declaration

I, John Mulwa Ndisya, hereby declare that this thesis is my original work. To the best of my knowledge, the work presented here has not been presented for a degree in any other Institution of Higher Learning.

John M. Ndisya, B.Sc _____ _____

Signature Date

This thesis has been submitted for examination with our approval as University Supervisors.

Ayub N. Gitau, PhD _____ _____

Signature Date

Duncan O. Mbuge, PhD _____ _____

Signature Date

## Dedication

I dedicate this work:

To God Almighty, my Father, my Lord and my Savior

To my family (Grandma Monicah Mulwa, parents Bernard Mulwa and Priscillar Ndisya, siblings Richard Kioko, Irene Mwikali, Benjamin Mwaka and Philip Mwongela)

To my fiancée Esther Makau

**Acknowledgement**

I would like to thank the University of Nairobi through the School of Engineering and the Board of Postgraduate Studies for awarding me a scholarship to undertake my studies. I am also greatly indebted to the Department of Environmental and Biosystems Engineering for allowing me to use their resources for my studies and research.

I express my sincere gratitude to Eng. Prof Ayub Gitau and Eng. Dr. Duncan Mbuge whom I was privileged to have as my research supervisors. They guided me during the research problem identification, assisted me to refine the research idea and saw to it that I produced this research thesis on time. They were committed in reading my work, positively critiquing it and in correcting me where I went wrong. Their encouragement and availability for consultation were simply second to none.

The support of Dr. Christian Thine in refining the research idea and Eng. Daniel Mutuli in providing me with literature material went a long way in assisting me produce a quality research proposal. I am grateful to Mr. Januaries Agullo for his assistance with statistics and statistical packages (R and SPSS); I also thank him for reviewing my research proposal and draft thesis. I also thank DEM Solutions Limited, through Mr. Ammar Khalid, for providing me with the license key to use EDEM Academic™ 2.7.0 in my research through the EDEM Academic Partner Program (EAPP).

My sincere gratitude also goes to Mr. Francis Wahome, Mr. B.A Muliro, Mr. Wamutitu and Mr. Macharia, technologists at the Department of Environmental and Biosystems Engineering for their guidance during field investigations and for their assistance in conducting the various laboratory tests required to support the research work.

# Numerical simulation of soil resistance in ripping: A case study of a sandy clay soil

**BY**

**Ndisya John Mulwa**

**F56/69345/2013**

## Abstract

In this study, a numerical model based on field experiments, laboratory experiments and simulation was developed to predict the soil resistance to ripping in a sandy clay soil. The study identified the soil and operational parameters that influence soil cutting and that are pertinent to the development of a discrete element model.

Field experiments were conducted to collect soil resistance datasets. Draft data was measured using the MSI 7300 digital dynamometer logging data directly to a laptop through the serial port. The ripper tines tested were attached to a tool carriage attached to the three point hitch of the towed tractor (i.e. gear lever in neutral position); the dynamometer was attached between the rear towed tractor and the front towing tractor via steel shackles.

A $2\times3\times4$ factorial experiment in a Completely Randomized Block design was the statistical technique used to investigate the effects of the operating speed, ripping depth and rake angle on the draft force requirement of a 5cm wide ripper tine. The rake angle was the blocking factor in four levels ($30^o$, $45^o$, $60^o$ and $75^o$), tillage depth in three levels (15, 25 and 45 cm) and operating speed in 2 levels (3 and 5 km/hr.). Four replications were used to give a total of 96 treatments.

The EDEM Academic™ software from DEM Solutions Limited was applied to simulate the soil resistance to ripping using the different ripper tines. The model was calibrated using the angle of repose test; the forces arising due to particle and boundary contact during simulation were calculated using an inbuilt contact constitutive relation and displayed using EDEM Academic™ inbuilt query feature.

The draft datasets obtained from the experiments and the simulation were subjected to Analysis of variance (ANOVA) and the student t-test; the coefficient of determination ($R^2$) was determined from linear regression to be 0.986 indicating a good degree of fit of the measured draft datasets to the predicted draft datasets.

ANOVA indicated that the rake angle, operating speed and ripping depth significantly influenced the value of the draft force at the 95% level of confidence. The draft force was found to decrease from a rake angle of $30^o$ to attain a minimum value at $45^o$ then increased to attain a maximum at $75^o$. The rake angle of $45^o$ was thus found to give the minimum amount of draft force while the rake angle of $75^o$ was found to give the maximum amount of draft force. The draft force increased linearly as the tillage depth and operating speed increased suggesting that they are directly proportional.

It was established that the discrete element method was applicable in modeling soil-tool interaction processes and thus could be applied in research activities, product development activities for rapid prototyping and in an actual farm setting to swiftly and reliably establish the expected draft forces and thus in extension aid in the establishment of energy requirements for a particular ripping operation.

**Key Words**: Soil resistance; discrete element method; numerical simulation; specific draft; rake angle; ripping depth; operational speed

## Table of Contents

## List of Figures

## List of Plates



## List of Tables

## Acronyms

| Acronym | Meaning |
|---|---|
| ACIAR | Australian Centre for International Agricultural Research |
| ANOVA | Analysis of Variance |
| ASTM | American Society for Testing and Materials |
| CAD | Computer Aided Design |
| CFD | Computational Fluid Dynamics |
| CIMMYT | Centro Internacional de Mejoramiento de Maíz y Trigo (International Maize and Wheat Improvement Center) |
| DEM | Discrete Element Method |
| FEM | Finite Element Method |
| JKR | Johnson, Kendall and Roberts |
| KENDAT | Kenya Network for Dissemination of Agricultural Technologies |
| kN | Kilo Newton |
| LAMMPS | Large-scale Atomic/Molecular Massively Parallel Simulator |
| LARMAT | Land Resource Management & Agricultural Technology |
| LIGGGHTS | LAMMPS Improved for General Granular and Granular Heat Transfer Simulations |
| MIMES | Multi-scale Integrated Models of Ecosystem Services |
| PFC | Particle Flow Code |
| RAM | Random Access Memory |
| SPH | Smoothed Particle Hydrodynamics |
| SPSS | Statistical Package for Social Scientists |
| TB | Terabytes |
| UDEC | Universal Distinct Element Code |
| YADE | Yet Another Dynamic Engine |

# CHAPTER ONE: INTRODUCTION

## 1.1 Background

Soil compaction, a challenge that many farmers worldwide face has been shown to reduce crop productivity in any agricultural system (Nawaz *et al*., 2012; Wiebe, 2003). Soil compaction is caused by various factors including machinery wheel traffic, prolonged use of the moldboard plow, eluviation of fine soil particles from the soil surface to a fine textured soil layer in the subsoil and the trampling by livestock during grazing prior to cultivation.

Linde (2007) observes that climate change, escalation of agricultural input prices and the reducing size of landholdings in the recent years has forced researchers to develop conservation agriculture to mitigate the negative environmental effects of conventional agriculture particularly soil erosion and the emission of carbon dioxide held in the soil to the environment. In spite of the major strides being taken towards conservation agriculture, soil compaction is still a dominant problem and thus breaking-up the compacted soil is still a major contributor to the input costs (Linde, 2007). Moreover, conventional agriculture is still practiced in many parts of the world; ripping is still one of the operations performed to alleviate soil compaction and loosen the soil before planting.

A ripper is a chisel-shaped agricultural implement that can be animal or tractor powered. The ripper breaks up and opens a narrow slot or furrow in the soil, about 15 to 50 cm deep. It is one of the tillage implements used in both conventional and conservation agriculture systems to alleviate soil compaction. Unlike a moldboard plow, the ripper loosens the soil without overturning and moving the soil clods, usually, farmers who want to circumvent plowing in minimum or reduced land preparation activities use rippers.

Ripping requires considerably high draft requirement that results into increased energy requirements. Furthermore, ripping is a time intensive operation performed before planting, its timeliness is thus an important factor in agricultural productivity and can interrupt planting activities if not timely performed. As a result, ripping operations require proper planning beforehand; farmers and farm managers require prior knowledge on the size of tractor and amount of fuel and lubricants required for ripping so as to provide sufficient financing (Moeenifar *et al*., 2013).

Equipment manufacturers have for a long time designed tillage tools on the basis of experience and development of prototypes which has worked well, however, Linde (2007) reports that "optimizing a tillage tool with prototype testing alone would require more finances and time due to the number of parameter combinations influencing its performance"; this has forced researchers to develop models to simplify the task. Several researchers have developed various models for predicting the forces on tillage tools for design purposes; nonetheless, these models have been developed from experiments for specific tools in specific circumstances and can thus not easily be used for tool optimization or the evaluation of the effects of different parameters of a tillage tool (Linde, 2007).

In recent times and with the advancement in technology, computing has influenced every sphere of human activities; computers have introduced speed and ease to tasks in many sectors including education, business, health, war and manufacturing among others. The design and optimization of tillage tools has not been bypassed by the dynamic developments in technology, with the advent of powerful computers, a number of numerical techniques have been developed to model tillage forces and the material failure resulting from their action. These techniques include the continuum methods like Finite Element Method, Smoothed Particle Hydrodynamics and Computational Fluid Dynamics and discrete methods such as the Discrete Element Method (Obermayr *et al*. , 2011).

A lot of research has been done on the development of tillage models based on the continuum methods, however, the treatment of soil as a continuum doesn't reflect the true nature of soil as we know it; consequently the continuum methods cannot sufficiently model the considerable soil displacements that occur during tillage. On the other hand, the Discrete Element Method was specifically formulated for handling problems involving granular material like soil; it can be applied to simulate the considerable soil movements involved in tillage as well as its reaction under vibratory loading (Linde, 2007).

### 1.2 Problem Statement and Justification

Tillage is one of the most power consuming land preparation operations conducted each season particularly in medium to large farms that extensively use tractors. Unfortunately, Marenya (2009) notes that the sustained increase in the price of fossil-based fuels and lubricants has fostered a tremendous increase in the cost of land preparation; this increase is generally passed on to consumers in the form of inflated food prices.

There is a genuine need to make soil tillage more energy efficient in order to sustain significant profit margins. Soil tillage now presents a challenge to farmers and equipment manufacturers more than ever; farmers are being forced to work within constrained budgets while machine manufacturers are struggling to optimize the energy efficiency and capital cost of their equipment to remain competitive in the marketplace.

An energy efficient tillage tool is that which accomplishes a particular tillage operation with reduced draft power requirement to overcome soil resistance; draft requirement is thus a reflection of the amount of soil resistance to a tillage tool. The prediction of draft requirement is an important undertaking in the design of tillage tools; it is however a "complex process due to the spatial variability of soil properties, the nonlinear and dynamic behavior of soil and the interaction between particles contact phenomenon such as slippage, particles re-arrangement due to stress and the flow that occurs at the interface zone between the soil and the tillage tool" (Asaf *et al*., 2007; Shmulevich, 2010).

Over time, several analytical, empirical and numerical models have been developed to predict the soil resistance for various tillage tools (Marenya, 2009); these models have worked within acceptable degrees of success. Nevertheless, the analytical models on tillage are almost always based on the passive soil pressure theory formulated by Terzaghi (as cited in Shmulevich, 2010) and require prior assumption on the soil failure pattern before the model can be developed; on the other hand, there is a serious drawback with empirical models as "they are limited to relatively simple geometries and trajectories of the working tool" (Martin Obermayr et al., 2011). These models are thus not versatile enough for tillage tool design and optimization.

This research utilized the numerical technique to develop a model for the soil-resistance of ripping in a sandy-clay soil and establish the optimal rake angle, cutting depth and operating speed to achieve reduced soil-resistance.

## 1.3 Objectives

### 1.3.1 Broad objective

To apply a numerical simulation model to predict the draft requirement of ripping in a sandy clay soil and establish the effect of the rake angle, cutting depth and operating speed on the draft force.

### 1.3.2 Specific objectives

The specific objectives were to;

1. Evaluate the numerical values of the tillage parameters pertinent to ripping
2. Apply, verify and validate a discrete element model using the values of the parameters identified in (1) above to predict the draft requirement
3. Establish the effect of the rake angle, cutting depth and operating speed on the draft force

## 1.4 Scope of the Study

This research was limited to numerical simulation of the draft requirement of ripping in a sandy clay soil. Four ripper tines with different rake angles were subjected to field tests under varying operating speeds and tillage depths.

The only soil tests conducted were those necessary in the development of the numerical simulation model; they included soil bulk density, angle of internal friction, cohesion, adhesion, soil textural analysis, moisture content and penetration resistance.

The model developed was only limited to capturing the horizontal forces (i.e. draft forces). The vertical and lateral forces were therefore not predicted. Moreover, the research was conducted in a sandy clay soil.

# CHAPTER TWO: LITERATURE REVIEW

## 2.1 Preamble

This chapter provides a review of past research efforts linked to this study. It includes a brief background on soil compaction, ripping and the effects of soil parameters, tool parameters and operating factors on soil failure. Further, the various approaches to modeling power requirements of tillage tools are presented.

## 2.2 Soil Compaction in Agriculture

Soil compaction is a form of physical degradation depicted by an increase in the soil's density and a corresponding decrease in the pore space as a result of applied loads. For engineering purposes such as the construction of a road, soil compaction increases the roadbed resistance to deformation and is thus desirable; however, soil compaction is undesirable in a farm setting as it reduces the infiltration capacity leading to increased surface runoff and the erosion of agricultural soils (Lull, 1959; Payne, 2008).

According to Payne (2008), soil compaction affects the physical, chemical and biological properties of the soil as well as hampering root growth. The initial effect on root growth is reduced nutrient uptake which in due course affects the entire plant (Lichtfouse, 2010). Indeed, research by Penn State Extension (n.d.) in tilled soils indicated yield losses in the first year due to severe compaction of about 15 percent due to residual effects of surface compaction. In the absence of recompaction, yield losses decreased to approximately 3 percent ten years after the compaction event.

Soil compaction is a problem in both conventional and conservation agriculture systems (Gitau and Gumbe, 2004). McGarry (as cited in Benites *et al*., 2005) considers soil compaction to be the worst form of land degradation resulting from conventional agriculture practices caused by agricultural tires and implements working in moist to wet conditions at which the soil is susceptible to deformation. Conservation agriculture has been reported to generally improve the soil physical condition by reducing mechanical disturbance of the soil by Losada *et al*., (2005) and Gitau and Gumbe (2004); however, Blanco-Canqui (2008) argues that soil compaction may actually increase with the conversion of conventional systems to conservation systems due to a lack of transient soil loosening by tillage operations particularly in no-till systems with poorly drained clay soils.

### 2.3 Ripping and Ripper Tines

A ripper is a chisel-shaped agricultural implement that can be animal or tractor powered. The ripper breaks up and opens the soil up to about 15 to 50 cm deep in both conventional and conservation agriculture systems to alleviate soil compaction.


**Figure 2.1: A gang of rippers held by tool carriage (Schmeiser Farm Equipment, 2014)**

Recent research has seen the development of advanced ripping mechanisms such as the vibratory ripper which utilizes a chain-gear mechanism. Linde (2007), reports that the use of a vibrating tillage tool is an effective method of reducing the draft force, he utilized the vibratory mechanism to test and model the effect of the vibration on the draft force of a sub-soiler. A different mechanism includes the use of an impact ripper that utilizes an hydraulic hammer to break even harder and rocky formations (Smith *et al*, 2001). These advanced ripping mechanisms, do however increase the overall energy consumption (Linde, 2007).

In practical farm operations, it is the norm to connect several ripper tines on a common carriage in various gang arrangements or with other tools such as scrapers, seeders, discs among others. Kasisira (2004) discovered that deep tilling once every number of years at the same depth actually increased the problem of compaction as a result of operating below the critical depth; he proposed an arrangement in which the tools are arranged in a tandem configuration.

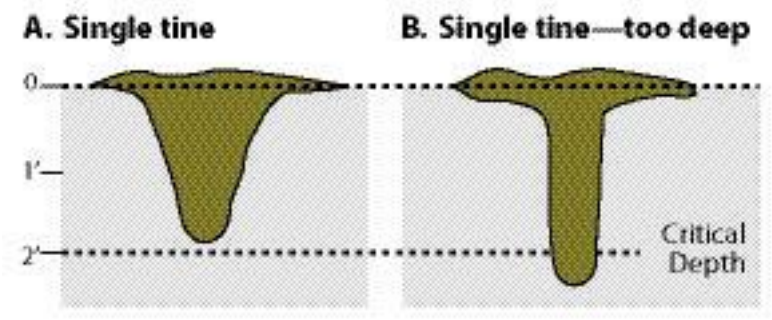


**Figure 2.2: The Critical Depth: Source (Armstrong, n.d.)**

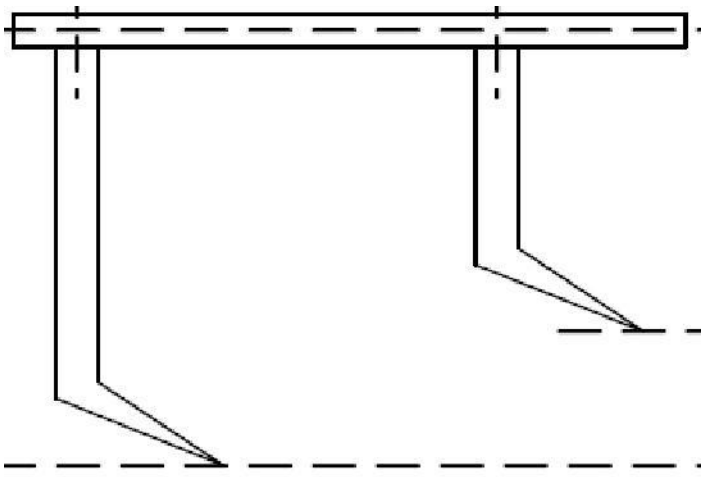

**Figure 2.3: Tools in tandem configuration: Source (Kasisira, 2004)**

The problem presented by the tandem arrangement is that, bigger and more powerful tractors might be required to draw the tools through the soil resulting into more energy consumption and a greater deal of soil compaction as a result of the heavier tractor. On the contrary, lighter tractors are being introduced by CIMMYT in partnership with ACIAR, KENDAT and the University of Nairobi to serve small-scale farmers in Kenya, these tractors, most of them two-wheeled, are technically unable to draw rippers in a tandem arrangement.

### 2.4 Influence of Soil, Tool and Operational Parameters on Soil Resistance

Tillage in an agricultural soil involves loading the soil until cracking patterns develop. According O'Callaghan *et al*. (as cited in Kasisira, 2004), the soil deforms both elastically and plastically when a force is applied to the tillage tool; the stress in the soil increases in the zone ahead of the surface of the soil-engaging element reaching a critical stress value where the soil fails. This has been confirmed by the Mohr-Coulomb failure criterion which

contends that a soil mass fails at the point where the shear stress reaches the shear strength of the soil (Raj, 2008).

The Mohr-Coulomb criterion postulates that the soil shear strength is a function of the soil cohesion and the soil-to-soil friction. The soil cohesion is dependent on the strength of the bonds between adjacent soil particles only and represents the maximum value of the shear stress when the normal stress is set to zero. However, soil-to-soil friction results from the interlocking of rough soil particles and is thus a function of the applied normal stress (Marenya, 2009).

The geometry of a tillage tool and the soil shear strength parameters control the shape of the failure plane that results. Kasisira (2004) reports that the average soil resistance to a tillage tool is approximated by the force needed to develop the initial failure plane. The failure of an agricultural soil is influenced by various factors including soil parameters, tool and operating parameters that have a direct bearing on the soil resistance experienced during passive tillage.

### 2.4.1 Effect of Soil parameters on Soil Resistance

The soil physical properties contributing to soil resistance include the moisture content, bulk density, texture, temperature, color and porosity (Marenya, 2009). According to Gill (1968), soil physical properties particularly the moisture content, bulk density and texture affect the mechanical behavior and shear strength of a soil.

According to Rose (2004), soil strength is generally reduced as it absorbs water due to a concurrent decrease in the cohesion and the friction angle. The moisture content affects the ability of a particular soil in a particular condition to resist or endure an applied force and hence directly influences the amount of soil resistance to tillage (Gill, 1968; Gitau *et al.*, 2006). Various techniques exist for establishing the moisture content in a soil, the simplest method being the gravimetric method where the water content is expressed as the ratio of the weight of water contained in a weight of dry soil.

The soil bulk density has been shown to be almost linearly related to the soil resistance measured by the penetrometric technique (Dedousis and Bartzanas, 2010). Soil bulk density is known to be a function of moisture content and the compactive effort, Chancellor (as cited in Marenya, 2009) observed that the changes in the amount of moisture within different soil depths influenced the soil bulk densities within such depths. Marenya (2009) therefore recommends that studies geared towards the quantification of soil resistance to tillage be conducted at a constant bulk density throughout the test layer.

### 2.4.2 Effect of tool and operating parameters on Soil Resistance

Godwin and O'Dogherty (2007) define a narrow tine as the one having a depth to width ratio of between one and six; very narrow tines have a depth to width ratio beyond six. Soil failure under the action of narrow tines is three dimensional in nature depicting two modes of failure at a certain critical tine depth ($d_c$) as postulated by Godwin and O'Dogherty (2007);

- Crescent failure near the soil surface and above the critical depth with soil moving forwards, sideways and upwards
- Lateral failure below the critical depth with the soil moving forwards and sideways only

The slenderness of a tillage tine has been reported to influence the location of the critical tine depth ($d_c$) which in turn dictates the maximum useful cutting depth of the tine. According to Kasisira (2004), operating the tine below the critical depth reduces soil pulverization, causes soil compaction while increasing the soil resistance to the tine; this was confirmed by McKyes *et al.* (as cited in Zadeh, 2006) who observed that the soil resistance and the degree of soil pulverization increased with the relative narrowness of the tillage tines.

Ghaly and Al-Suhaibani (2010) studied the effect of the cutting depth and operating speed on the performance of a medium sized ripper in a sandy soil. Their findings revealed that increasing the cutting depth and/or the operating speed increased the soil resistance to ripping. Owen (as cited in Ghaly and Al-Suhaibani, 2010) investigated the force to depth relationship of a ripper tine with three different wing types in a compacted clay loam soil and found the vertical force on the tine to increase linearly with the cutting depth; the horizontal force, moment and total force increased quadratically with the cutting depth.

In their research to establish the effect of the rake angle of a ripper on the power requirements while working in a clay loam soil, Tong and Moayad (2006) found out that the soil resistance on a tool decreased with increase of the rake angle from $15^o$ to $45^o$ where it attained a minimum value and then increased to a maximum value at a rake angle of $75^o$. To achieve less soil resistance, high cutting efficiency and excellent soil pulverization during ripping, Zadeh (2006), recommends that the tool should have a rake angle of about $30^o$ and should be fairly narrow with a depth to width ratio of at least two.

## 2.5 Modeling soil resistance to tillage

The global demand for energy has of-late risen to considerably high levels due to accelerated industrialization and population growth. The high demand for energy is believed to be one of the causes of the widespread conflicts and wars currently being waged in various parts of the world. With industrial development, more sophisticated machinery requiring higher amounts of energy have been developed for various agricultural functions.

Much of the energy required for agricultural activities is consumed by tillage to provide sufficient draft to overcome the soil resistance and power soil pulverization processes. Newton's third law of motion states that "to each action there is always an equal and opposite reaction"; the interpretation of this is that the soil resistance to a tillage tool will be of an equivalent magnitude to the measured or predicted draft on the tool after subtracting any rolling resistance of the prime mover.

Zadeh (2006) observed that the energy consumed in a tillage operation is a function of the soil type and condition, tool parameters and operating parameters. Over the years, a number of researchers have developed analytical, empirical and numerical models to predict the draft required by various tillage tools; these models combine the factors above into a mathematical equation or a computer model to predict the draft.

### 2.5.1 Analytical models

A lot of research has been done on the prediction of the forces acting on a simple tool and the soil failure developed in the process (Kasisira, 2004; Marenya, 2009; Zadeh, 2006). Limit equilibrium analysis has been analytically employed to describe soil failure under tillage and force prediction models based on Terzaghi's (as cited in Kasisira, 2004) passive earth pressure theory. Two dimensional models have been developed for wide tillage tines (depth to width ratio less than 0.5) while three dimensional models have been developed for narrow (depth to width ratio between 1 and 6) to very narrow tines (depth to width ratio greater than 6).

Payne (1956) was the pioneer of three-dimensional force prediction for inclined tillage tools. He made an assumption of the failure zone for tines with a width/depth ratio less than one by observing the upward displacement of the soil ahead of the tillage tine (Zadeh, 2006). This model was improved by Osman (1964) by introducing soil properties, tool rake angle and tool surface roughness to the force expression by employing dimensional analysis.

A force prediction model was developed by O'Callaghan and Farrelly (1964) as an extension to Payne's (1956) work. It is reported by Marenya (2009) that the influence of the side crescents for soil failure above the critical depth and the forces resulting from adhesion and soil interface friction were not taken into account in developing the model, further, Zadeh (2006) notes that the model underestimated the draft force when a very hard soil was encountered; he attributed this weakness to the nature of the assumptions made while developing the model.

Hettiaratchi and Reece (1967) developed a three dimensional model for soil failure based on the passive earth pressure theory. They assumed that the failure configuration involved forward and transverse failure regimes (Grisso and Perumpral, 1985). The total force on the tools was reported to be the sum of the forces for the forward and transverse failure. Even though this model captures the soil properties, soil-metal frictional properties and the tool geometry (Marenya, 2009), Grisso and Perumpral (1985) indicate that it tends to predict the draft force above the expected range.

Godwin and Spoor (1977) studied the soil failure mechanism under the action of narrow tines with various degrees of slenderness. A circular shape was proposed for the soil failure crescents on the soil surface and the sides of the tines to establish the volume of soil displaced by the tine (Zadeh, 2006). The soil failure in front of the tool was hypothesized to be a wedge and the equation developed by Hettiaratchi and Reece (1967) for wide tines was utilized to obtain the draft from the centroid of the wedge.

Studies by McKyes and Ali (1977) on the cutting of soil by narrow blades produced a three-dimensional force model similar to that of Godwin and Spoor (1977). They however developed an equation to establish the rapture distance in terms of a failure angle and the soil and tool parameters; this eliminated the need of having prior knowledge on the rapture distance for establishing the forces on the tine. The draft prediction equation developed was the sum of the forces from the center wedge and the side crescents. However, Grisso and Perumpral (1985) report that the McKyes-Ali model doesn't predict the lift force on the tool accurately.

Perumpral *et al.* (1983) developed a soil-tool equation based on limit equilibrium analysis. This model was based on the Godwin and Spoor (1977) and McKyes and Ali (1977) models but the side crescents adjoining the center wedge were substituted with two sets of forces acting on the faces of the center wedge (Grisso and Perumpral, 1985). The prediction

equation was given as a sum of the forces acting on the horizontal and vertical directions of the center wedge. Swick and Perumpral (1988) improved the work done by Perumpral *et al* (1983); they formulated a three dimensional soil cutting model that took into account the tool dynamic effects. Even though this model utilized some assumptions that overestimated side crescent dimensions (Zadeh, 2006), it gave a sufficient prediction of the forces acting on a narrow tine (Kasisira, 2004).

A dynamic soil cutting model was developed by Zeng and Yao (1992) taking into account the acceleration and strain rate effects to predict the forces on both wide and narrow tines. Apart from a prior knowledge of shear strain at soil failure to establish the shear failure boundary, this model was otherwise similar to that developed by McKyes and Ali (1977).

### 2.5.2 Numerical models

Various numerical models have been developed to predict the forces acting on tillage tools. These models have been introduced into the field of tillage science due to the recent advances in computing power (Zadeh, 2006). Most of the numerical models developed in tillage research have been formulated using the Finite Element Method (FEM), Smoothed Particle Hydrodynamics (SPH), Computational Fluid Dynamics (CFD) and the Discrete Element Method (DEM).

FEM can be used without a prior assumption of the soil failure pattern presenting the possibility of modeling tillage activities that use tools of various shapes (Kasisira, 2004). Furthermore, FEM presents an advantage over the analytical methods discussed above if a constitutive relation for the soil is provided. However, Marenya (2009) reports that the constitutive relation for agricultural soils is not yet fully understood and thus FEM has limited applicability in precision modeling and optimization of tillage tools.

SPH is one of the continuum simulation approaches which use a mesh free based algorithm unlike FEM. Urbán *et al.* (2002) used the SPH method to assess its applicability in soil-tool interaction simulation, they reported that SPH requires less computational resources and time to configure and run a simulation. SPH however always overestimated tillage forces and thus more research is required to provide accurate material models for calibration.

Karmakar (2005a) reports that the study of soil mechanical behavior from a Viscoplastic fluid flow perspective using CFD is useful to tillage dynamics. He successfully modeled soil failure using a Bingham model in CFD to depict soil plastic failure with respect to the yield stress. However, Karmakar *et al.* (2009b) experimentally validated a CFD model for a narrow

tillage tool and discovered that it over predicted the draft force. CFD predictions for higher operating speeds and depths were found to be significantly different from the experimental values.

According to Shmulevich *et al.* (2007), the complexity of modeling the actual soil-tillage interaction behavior becomes more profound when dynamic effects are taken into account; a better understanding of soil translocation during tillage is thus required to forecast the redistribution among soil particles (Shmulevich *et al.*, 2007). DEM provides an adept alternative for modeling soils and their interaction with both rigid and flexible bodies thus depicting the non-linearity in soil behavior; with good computing resources, DEM provides an easy way to set-up, calibrate and run simulations; DEM is thus a promising way to model the actual soil behavior particularly in tillage without the limitation of the other numerical methods and may serve as a tool for optimization of the design process (Asaf *et al.*, 2007).

Over the past few years, several researchers have reported the ability of DEM in simulating the micro-mechanics of the dynamic behavior of particles that form the material in various engineering and science applications. Sitharam (2000) presented the theory of DEM and some of its applications in engineering; he reported that DEM simulated deformation mechanisms in particulate media more reasonably than the continuum methods, it was detailed enough to develop and validate constitutive relations of particular materials using their appropriate particle properties, sizes, shapes and gradation.

Shmulevich *et al*. (2007) investigated the interaction between soil and a wide cutting blade using DEM and obtained a good correlation between the model results and experimental results. Linde (2007) developed a DEM model to optimize a vibratory subsoiler and quantify the draft reduction caused by the vibrating mechanism; he concluded that DEM was able to model the vibratory subsoiler mechanism for its design and optimization. Obermayr *et al.* (2011) developed a discrete element model that successfully reproduced the variations of the draft force for various cutting widths and depths for the calculation of soil-cutting forces in cohesionless granular material. (Okayasu *et al.*, 2010) established that the soil cutting behavior by a plow was controlled by soil conditions, tillage depth and tillage speed. It is thus evident that DEM is capable of reliably modeling the soil-tool interaction during tillage; this underscores its applicability in modeling the draft requirement during ripping.

## 2.6 Summary of the Literature Review

Soil compaction, a form of physical degradation depicted by an increase in the soil's density, reduces the infiltration capacity leading to increased surface runoff and soil erosion; this has a consequential effect of reducing crop productivity. Tillage operations, including ripping, are thus conducted in agriculture to alleviate soil compaction. However, ripping below the critical depth has been reported to increase the problem of compaction.

Various soil, tool and operational parameters are known to influence the process of soil – tool interaction during any tillage operation; the soil physical properties contributing to soil resistance include moisture content, bulk density, texture, temperature, color and porosity. Moreover, the tool width, operating depth, shape, rake angle and operating speed have been found to influence the soil resistance to tilling and consequently the draft requirement. Research has shown that increasing the tool width, operating depth and operating speed results to an increase in the soil resistance.

Over time, several analytical, empirical and numerical models have been developed to predict the soil resistance to various tillage tools. These models have worked within acceptable degrees of success. Nevertheless, the analytical models on tillage are almost always based on the passive soil pressure theory formulated by Terzaghi and require a prior assumption on the soil failure pattern before the model can be developed. Numerical modeling is a fairly novel approach developed to overcome the challenges of the analytical and empirical models; numerical models have been introduced into the field of tillage science due to the recent advances in computing power; they have been applied to solve problems in many scientific fields.

# CHAPTER THREE: THEORETICAL FRAMEWORK

## 3.1 Preamble

The discrete element method (DEM), also referred to as the distinct element method, is a numerical technique applied to establish the forces within and motion of a system consisting of numerous particles often of a small physical size.

The history of the discrete element method dates back to the nineteen seventies where it was first used to solve problems in rock mechanics. The initial application of this technique was envisaged by Cundall (as cited in Huang, 2010) in 1971; he developed a computer code to predict the progressive failure of a discrete mass. In 1979, Cundall and Strack (1979) developed the first functional computer program called BALL to model forces and motion in granular assemblages, since then, numerous studies on this method have been published.

Today, DEM has gained worldwide popularity and application in solving engineering problems involving granular materials in the oil and gas industry, manufacturing, agriculture, mining and space studies. DEM has been implemented in various open source and commercial modeling software including EDEM®, PFC, Yade, MIMES, LAMMPS, LIGGGHTS, Pasimodo, UDEC and SAMADII among others.

## 3.2 Fundamentals of Discrete Element Modeling

The calculation cycle in a typical Discrete Element Model (DEM) formulation follows the scheme shown in Figure 3.1. The DEM calculation cycle usually begins by supplying particle and geometry information that includes the particle radius and packing density. The scheme then generates particles and fills them in a geometry herein referred to as a 'Virtual Box'. At the start, the positions of the particles and the geometry are known; the scheme then executes the process of contact search and detection from the known positions of the elements, any particle overlaps are thus detected. By applying the Newton's law of motion, the resulting contact forces (i.e. particle to particle and particle to geometry) are calculated. The contact forces are entered into the law of motion for every particle and the velocity and acceleration of the particles are obtained, from the established values the new positions of the particles and the geometry in the current time-step are found. This calculation cycle is iterated for each time-step until the deformation of the material under consideration is simulated.

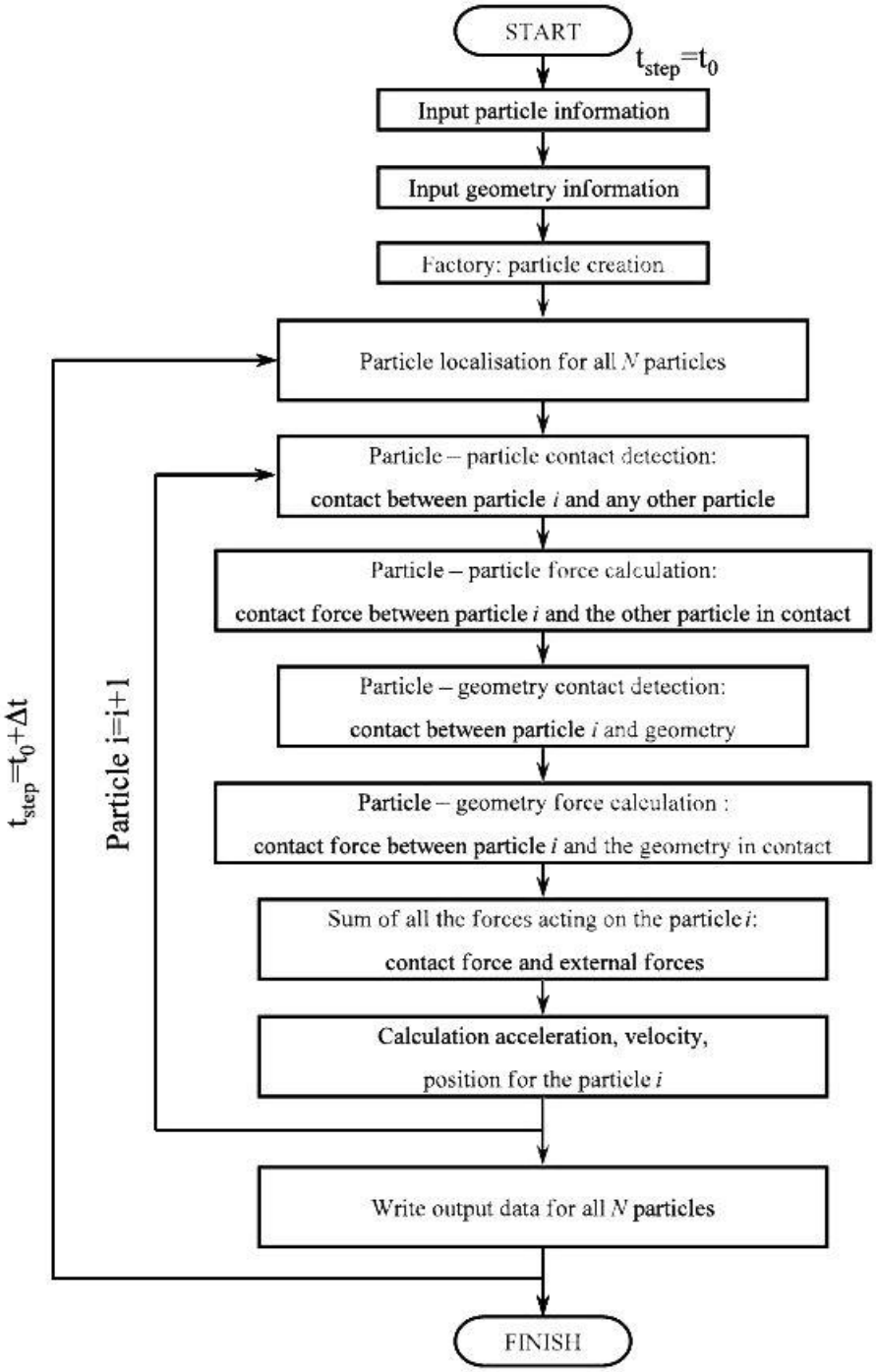


**Figure 3.1: Framework for the DEM Calculation cycle. Source (Marigo, 2012)**

### 3.2.1 Model Geometries

The commonly used geometries to represent particle shapes are the disc-shape and spherical-shape; these are employed in 2-dimensional and 3-dimensional models respectively. The use of simple particle geometries in discrete models is informed by the need to use as few parameters as possible which reduces contact detection time and significantly cuts down the required computational effort. However, the use of simple particle geometries causes

excessive particle rotation; the degree of particle rotation can be reduced by forming particle clusters that can be ellipsoidal or polygonal thereby increasing the angularity of the material.

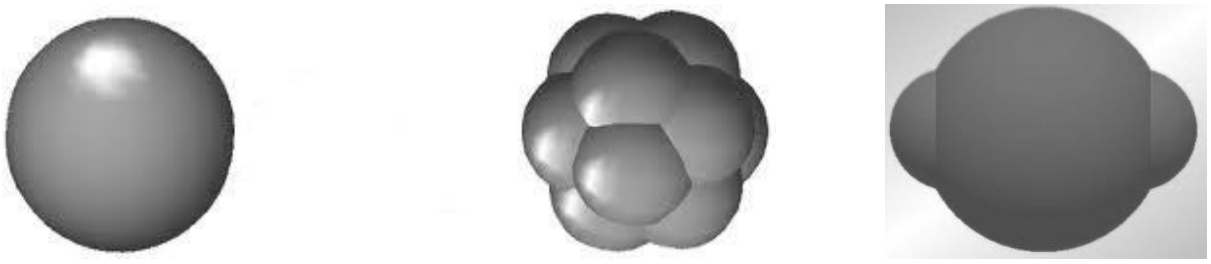

**Figure 3.2: Typical particle primitives (DEM Solutions Limited, 2014)**

There are two options for creating any other geometry or surface included in the model; the wall geometry or 'Virtual Box' which holds the particles is of a cubic or cuboid shape and is created using in-built geometry tools in EDEM Academic™. Other geometries that interact directly with the particles during simulation can take any arbitrary shape; basic shapes can be created using the in-built tools but more complex shapes can be created in third party CAD software and brought into the modeling environment using the in-built CAD-import option, as such, EDEM Academic™ is loosely coupled to various CAD software to enable independent geometry development.

### 3.2.2 Modeling Approaches in DEM

There are two approaches to modeling in DEM; hard particle approach and soft particle approach. The hard particle approach assumes that particles are perfectly rigid, they do not deform during collision and given the same initial conditions, the final results will always be the same. This approach is used to model a loose or dilute particle assemblage.

The soft particle approach, the particles are allowed to deform during collision resulting in overlap or penetration of the particles. In this approach, the Newton's laws of motion are applied to model the motion of each particle. This approach is used to model dense or packed particle assemblages such as soil and powder masses and will thus be used in this research.

### 3.2.3 The Equations of Particle Motion

The motion of particles is as a result of forces and moments acting at the center of mass. The translational and rotational motion of the center of mass defines the motion vectors at that point. The Newton's second law of motion (Equation 3.1) relates the translational motion to the resultant force (Ardic, 2006; Majidi, 2012).

$$F = m.\left(\ddot{\vec{x}} - \vec{g}\right) \tag{3.1}$$

where,

$F =$ resultant force,

$m =$ mass of the particle,

$\vec{\ddot{x}} =$ acceleration vector,

$\vec{g} =$ gravitational acceleration vector.

According to Hibbler (as cited in Majidi, 2012), the rotational motion is described by the 3-dimensional Euler equations if the local coordinate system is assumed to be oriented along the principal axes of inertia.

$$\begin{aligned} M_1 &= I_{11}\dot{\omega}_1 + \omega_2\omega_3\left(I_{33} - I_{22}\right) \\ M_2 &= I_{22}\dot{\omega}_2 + \omega_1\omega_3\left(I_{11} - I_{33}\right) \\ M_3 &= I_{33}\dot{\omega}_3 + \omega_1\omega_2\left(I_{22} - I_{11}\right) \end{aligned} \tag{3.2}$$

where: $I_{11}, I_{22}$ and $I_{33}$ are the principal mass moments of inertia, $\dot{\omega}_1, \dot{\omega}_2$ and $\dot{\omega}_3$ are the components of angular acceleration and $M_1, M_2$ and $M_3$ are the components of the resultant moment.

For spherical particles, the center of mass occurs at the center of the particle and thus the principal moments of inertia are equal at that point. Consequently, the above equations of rotational motion can be simplified as follows;

$$M = I\dot{\omega} = \frac{2}{5}m\dot{\omega}R^2 \tag{3.3}$$

where: $R =$ radius of the sphere

Itasca (as cited in Ardic, 2006) reports that for a small time step, $\Delta t$ in which the accelerations can be taken to be constant within the time step, the particle motions can be obtained from the equations of motion with the velocity terms being calculated at the center of the time step, $\Delta t/2$ as follows;

$$\vec{\ddot{x}}_t = \frac{1}{\Delta t}\left(\vec{\ddot{x}}_{t+\Delta t/2} - \vec{\ddot{x}}_{t-\Delta t/2}\right) \tag{3.4}$$

$$\dot{\omega}_t = \frac{1}{\Delta t}\left(\dot{\omega}_{t+\Delta t/2} - \dot{\omega}_{t-\Delta t/2}\right) \tag{3.5}$$

The resulting velocities for the succeeding time step evaluate to the following;

$$\ddot{\vec{x}}_{t+\Delta t/2} = \ddot{\vec{x}}_{t-\Delta t/2} + \left(\frac{F_t}{m} + \dot{g}\right).\Delta t \tag{3.6}$$

$$\dot{\omega}_{t+\Delta t/2} = \dot{\omega}_{t-\Delta t/2} + \left(\frac{M_t}{I}\right).\Delta t \tag{3.7}$$

The final position of the particle is given by the equation 3.8;

$$\vec{x}_{t+\Delta t} = \vec{x}_t + \dot{\vec{x}}_{t+\Delta t}.\Delta t \tag{3.8}$$

The values of $F_{t+\Delta t}$ and $M_{t+\Delta t}$ to be used in the succeeding time step are calculated from the contact constitutive law.

### 3.2.4 Iteration time step

A stable iteration time step is that which results to less computation time while maintaining solution stability (Ardic, 2006). To maintain a maximum particle overlap distance while observing the stable time step for highly dynamic simulations, the critical contact time is given by;

$$t_{critical} = 2.9432.\left(\frac{25.\gamma.m^2}{64.\Delta V}\right)^{\frac{1}{5}} \tag{3.9}$$

where: $\gamma = \frac{9}{16R}\left(\frac{1-\nu}{G}\right)^2$ , $\Delta V$ is the relative velocity at contact

Ardic (2006), considers a time step of about 10 to 20% the above critical contact time to be appropriate.

### 3.2.5 Contact Constitutive Law

The contact constitutive law is a relation which enables the determination of the forces arising due to two or more interacting particles. Several constitutive relations exist for both spherical and disc-shaped particles; a suitable constitutive relation enables accurate description of particle collision phenomenon. A model of a mass without initial cracks is shown in Figure 3.3.

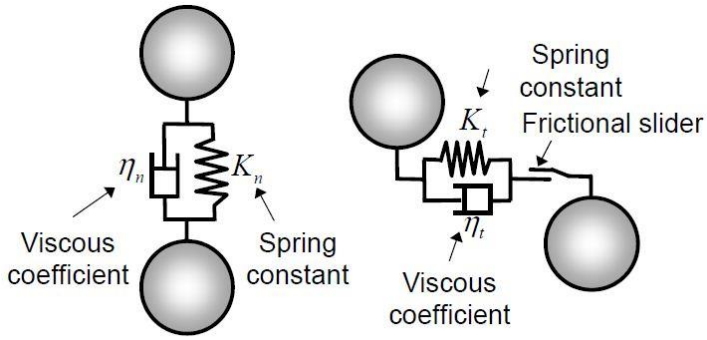


**Figure 3.3: Conceptual Discrete Element Model. Source (Okayasu *et al*., 2010)**

In Figure 3.3, the spring element represents the normal force which can either be tensile or compressive with a linear elastic behavior relating force and displacement. The dashpot element represents viscous damping between the particles while the sliding frictional slider represents shear force which too has a linear elastic behavior. According to Okayasu *et al*. (2010), a parallel bond exists between two particles in contact, this bond is capable of transmitting both forces and moments; however there is a critical value which if exceeded by either the tensile stress or shear stress between the particles the parallel bond breaks.

Ardic (2006) mentions that the contact forces are proportional to the contact area as opposed to the overlap distance and thus this relation is non-linear. The model is described by the following equations;

$$F_n = \frac{4}{3}.\overline{\mathrm{A}}.\sqrt{\overline{R}}.x_n^{3/2} \tag{3.10}$$

$$F_t = 8.\overline{\mathrm{B}}.\sqrt{\overline{R}.x_n}.x_t \tag{3.11}$$

where: $F_n$ and $F_t$ are normal and tangential forces as contact, $x_n$ and $x_t$ are normal and tangential overlap distances at contact, $\overline{\mathrm{A}} = \frac{A_1.A_2}{A_1 + A_2}$, $\overline{\mathrm{B}} = \frac{B_1.B_2}{B_1 + B_2}$, $\overline{R} = \frac{R_1.R_2}{R_1 + R_2}$,

$A = \frac{E}{1-\nu^2} = \frac{2.G}{1-\nu}$, $B = \frac{E}{2(1+\nu).(2-\nu)} = \frac{G}{2-\nu}$, $R =$ Radius of particle, $E =$ Young modulus of particle, $G =$ Shear modulus of particle, $\nu =$ Poisson's ratio of particle

### 3.3 EDEM Academic™ Software

#### 3.3.1 A general Overview of EDEM Academic™

EDEM Academic™ is a DEM software developed and distributed by DEM Solutions Limited to assist students and researchers develop models to simulate the behavior of particle systems under a variety of loading conditions. EDEM Academic™ provides an easy to use Graphical User Interface, parallel processing capabilities, extensive customization through an Application Programming Interface and built-in contact models.

EDEM Academic™ has been extensively used in simulation studies in rock mechanics, bearing capacity problems, bulk material handling, food processing and traction devices; this software will thus be used in this research to simulate soil-cutting by a passive ripper.

EDEM Academic™ graphical user interface makes it easy to set-up a model comprising of a particle system and various geometries. The initial set-up screen is the EDEM Creator® in which the particle and geometries are specified; the next stage is to set-up and run simulation parameters in the EDEM Simulator®; results can then be viewed and analyzed in EDEM Analyst® or exported to a spreadsheet program for further analysis.

#### 3.3.2 EDEM Creator®

The creator, also known as the pre-processor (DEM Solutions Limited, 2014), enables the user to build the structure of the model. The key functions provided by the creator include the following;

1. **On the globals tab**
   i). Selecting the units of choice from a selection of SI and MKS unit
   ii). Selecting and prioritizing the contact model from a selection of Hysteretic spring, Hertz-Mindlin with JKR, Linear cohesion, Linear spring, Hertz-Mindlin with Bonding, Hertz-Mindlin (no slip) and Hertz-Mindlin (no slip) with RVD Rolling friction.
   iii). Defining the mode of particle to particle and geometry to model interaction i.e. Coefficient of Restitution, Coefficient of Static Friction and the Coefficient of Rolling Friction
   iv). Creating model materials from scratch or selecting from the materials database. The properties of the materials that are then specified include; Poisson's ratio, Shear modulus, Density and Work function.

**2. On the Particles tab**

i). Creating the base particle shape

ii). Defining the particle properties including; radius, contact radius etc.

iii). Calculating the particle properties that include; position, mass, volume and moment of inertia.

**3. On the Geometry tab**

i). Creating geometry from scratch of the shape polygon, cylinder or box.

ii). Importing a preexisting geometry from a CAD software in the formats .stl, .stp, .iges or .step

iii). Defining the dimensions of the geometry and repositioning it

iv). Specifying the geometry properties such as material, nature (physical or virtual) and motion dynamics (translational, rotational etc.)

v). Specifying the model domain

**4. On the Factories tab**

i). Creating a particle factory (i.e. a polygonal plate from which particles will be created)

ii). Specifying the type of the factory (dynamic or static)

iii). Specifying the total number or the total mass to be produced per unit time

iv). Setting-up the factory parameters in the parameters section i.e. type, size, position, velocity, orientation and angular velocity.

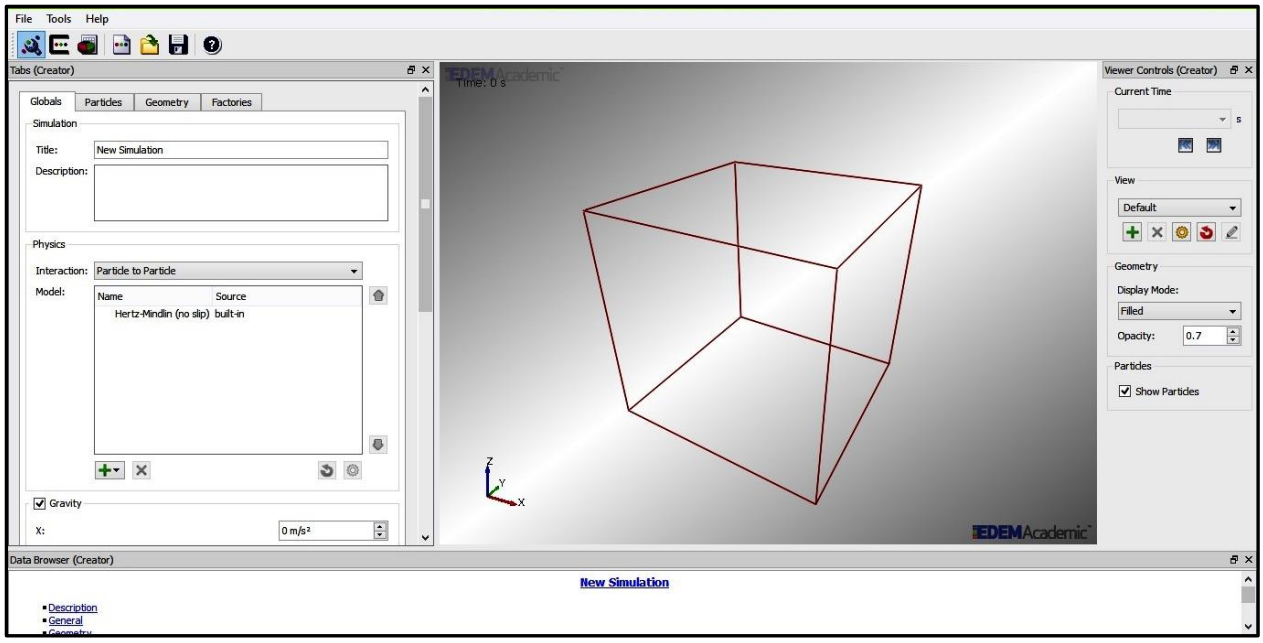


**Figure 3.4: Screen grab of EDEM Academic™ Creator® showing the Globals Tab**

### 3.3.3 EDEM Simulator®

The simulator, also referred to as the solver (DEM Solutions Limited, 2014), facilitates the setting-up of simulation parameters and running an actual simulation. The specific tasks that the simulator performs are as follows;

i). Setting the simulation time step (usually 20% of the Raleigh time step)
ii). Setting the total simulation time and data write-out frequency
iii). Setting the grid options
iv). Setting the view settings
v). Running the simulation

Of particular importance while setting-up a simulation is the speed of the simulation; various factors determine at what speed a simulation runs and how much time it takes to do so;

a) The number of cores on the computer in use; EDEM Academic™ has a parallel processing capability where it can be run on 2, 4, 8 or more cores; the greater the number of cores, the more the computational power and the faster the simulation
b) The selected mode of simulation; EDEM Academic™ can be run on a single file basis or on a batch file mode; the batch file mode makes it possible to run several files within a period of time without interrupting the simulation; the batch file mode thus runs the simulation faster than the single file mode

c) The type of data being written out; the user can select only a particular set of data of interest to be written out; this then reduces the resource demand on the system making it run at a faster rate

d) The specified data write-out frequency; the lower the frequency, the faster the simulation

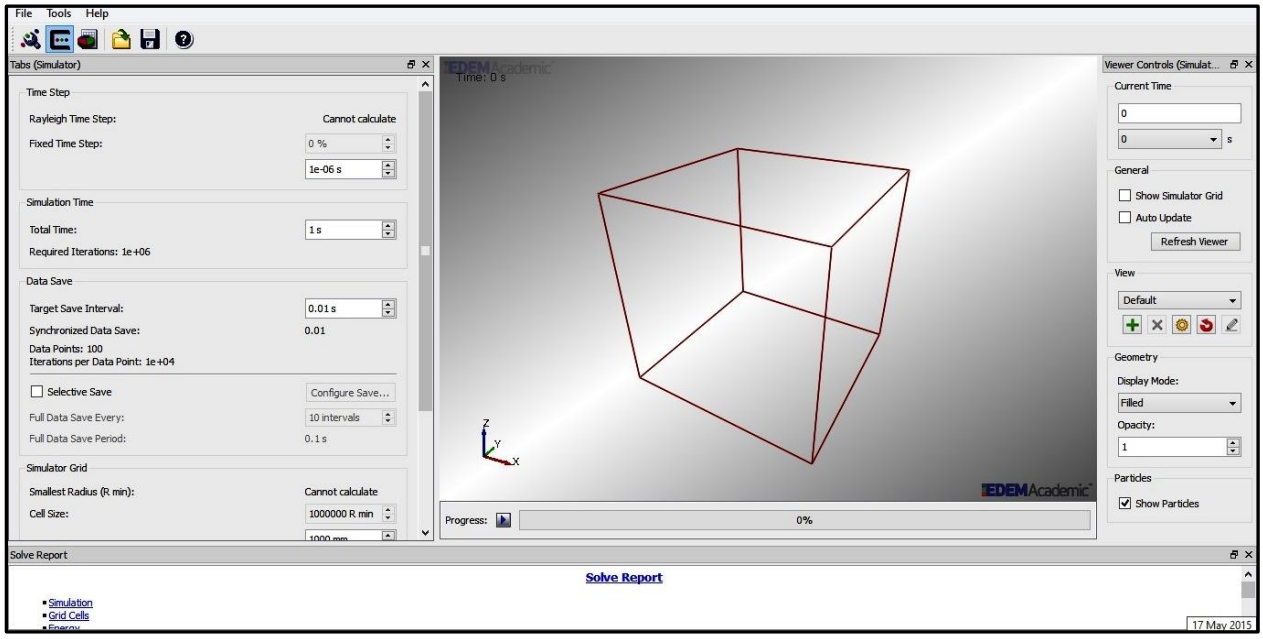


**Figure 3.5: Screen grab of EDEM Academic™ Simulator®**

### 3.3.4 EDEM Analyst®

The analyst, also known as the post-processor (DEM Solutions Limited, 2014) is used to review, examine and analyse the results of the simulation. It performs a variety of functions necessary to help the user make sense out of the results; such functions include clipping, colouring, measurements (using a ruler or protractor), querying among others.

The query functionality of EDEM Analyst® enables the user to export the simulation results in a format compatible with common spreadsheet software such as Microsoft excel; at that point, the user can then perform data cleaning, statistical treatment and graphing.

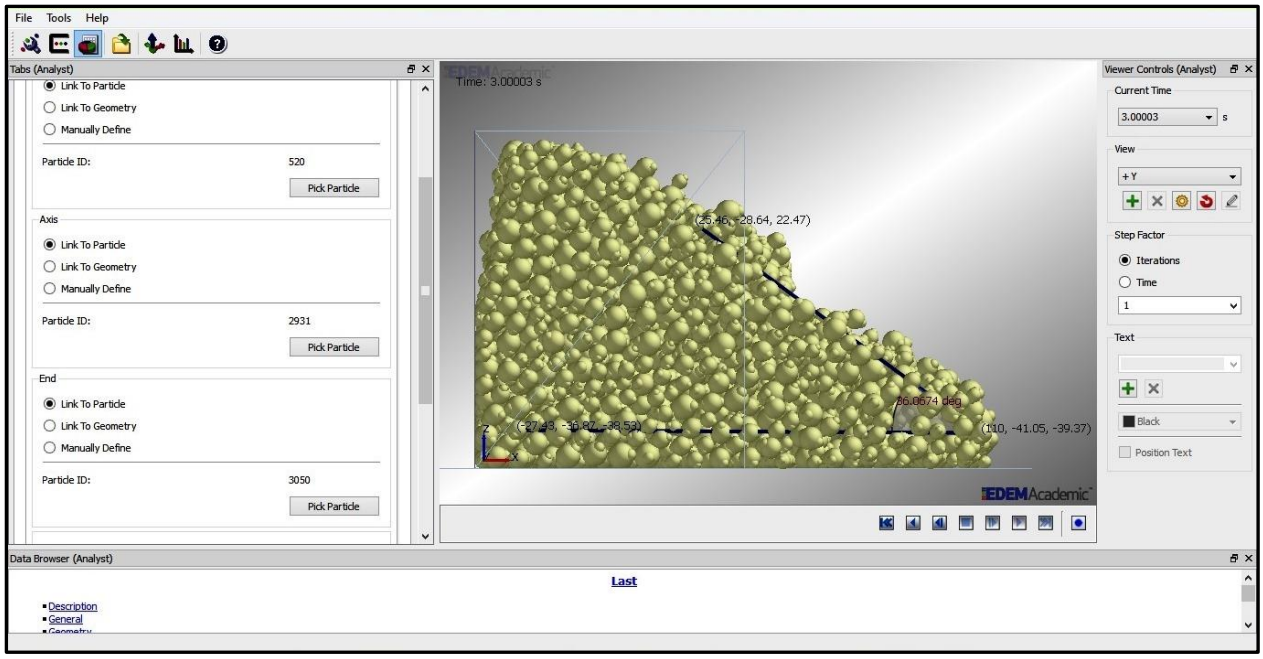


**Figure 3.6: Screen grab of EDEM Analyst® showing the Model Tab and Angle of Repose**

### 3.3.5 Relevant Contact Models in EDEM Academic™

A contact model describes the behavior of particles after making contact with neighboring particles or geometry section (DEM Solutions Limited, 2014). There several contact models available for use in EDEM Academic™;

i). **Hertz-Mindlin model (no slip)**: this is the default contact model in EDEM Academic™, its strength lies in its simplicity but has been reported by Milovac (2009) to over predict shear modulus due to its no-slip assumption; it however precisely predicts the bulk modulus.

ii). **Hertz-Mindlin with JKR Cohesion:** this model allows users to represent the cohesive nature of fine and moist materials.; it is particularly important in recreating the effect of moisture content on the bulk flow of materials such as iron ore or wet grains (DEM Solutions Limited, 2014). This model was extensively applied in this research.

iii). **Moving Plane model:** this model simulates the in-plane motion of a geometry section when contacted by a particle (DEM Solutions Limited, 2014).

## 3.4 Bulk Material Parameter Calibration

When modeling bulk materials, the DEM model must be calibrated to account for the bulk behavior of the material predominantly the irregular shapes of the soil particles and the variation of the soil properties. It is challenging to specify the granular shapes and properties

of soil with any DEM software, in some instances simplistic approaches to calibrating material behavior makes the model produce unrealistic results and thus this task must be done with rigorous experimental tests in a controlled environment to accurately reproduce materials properties and behavior.

For a DEM model to be calibrated there is a need to establish the micromechanical deformability parameters (Young's modulus, Shear modulus, Poisson's ratio) and strength parameters (i.e. cohesion, angle of internal friction) of the material particles. Calibration of a DEM model is an iterative process that requires an initial educated guess of the micromechanical parameters; they are then adjusted through sensitivity analysis and optimization techniques until the micromechanical properties give a response that matches the macromechanical properties of the bulk material.

A common approach to calibrating the bulk material in EDEM Academic™ for certain application is the use of the angle of repose test. For comparison purposes, the angle of repose test is replicated in EDEM Academic™; several instances with different values of Surface Energy value, Coefficient of Restitution, Coefficient of Static Friction, Coefficient of Rolling, Poisson's ratio, Shear modulus, Density and Work function are simulated in batch mode; at the completion of the simulation, the angle of repose in measured using the EDEM Analyst® protractor tool; the parameter combination that gives a value of the angle of repose similar to the physical test is deemed the true calibration set for the model.

### 3.5 Experimental Validation of Discrete Element Models

Models created using DEM methodology require to be experimentally validated. Depending on the application, different researchers have used different methods for this purpose. Huang (2010) while modeling railroad ballast using DEM used a model rail track to provide validation data; Obermayr *et al*. (2013) while investigating the reaction forces in excavation tools collected actual field data from excavation tests to assist them validate their DEM model.

Several researchers have also conducted studies in soil-bins to validate their DEM models. Linde (2007) used a combination of both field data and soil-bin studies to validate his DEM model of a vibratory subsoiler tine. Asaf *et al.* (2007) and Shmulevich *et al.* (2007) collected validation data from soil-bin studies for their DEM models of soil cutting blades.

# CHAPTER FOUR: MATERIALS AND METHODS

## 4.1 Description of the Study Area

The study was carried out in the University of Nairobi Field Station at Upper Kabete campus which lies at 1°15'S and 36°44'E at an altitude of about 1940 meters above sea level.

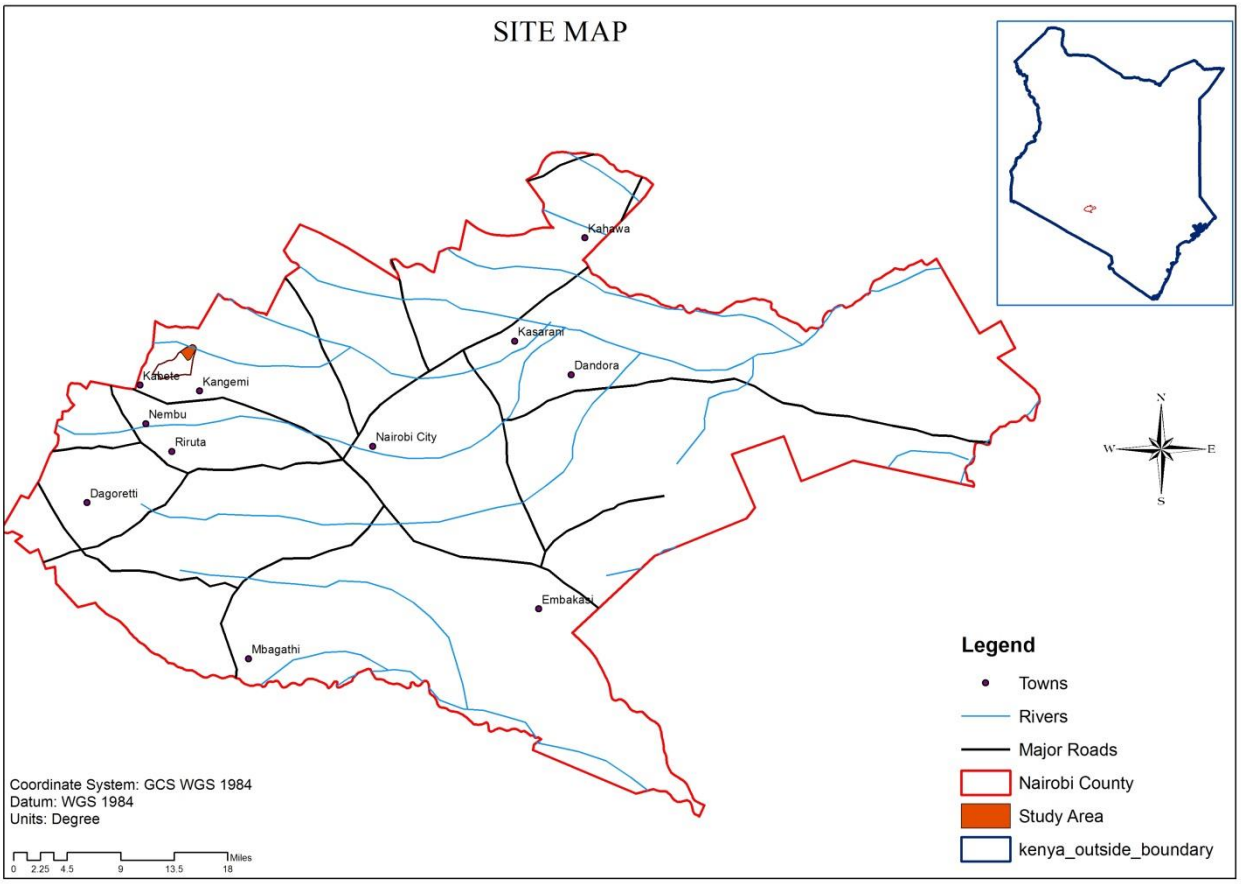


**Figure 4.1: Map showing the study area**

The soils and the climate of the area are reported by Karuku *et al*. (2012) to be representative of the Central Kenya Highlands. Gachene *et al*. (2000) also mentions that the soil at the site is a humic Nitisol with no surface crusting. The field station farms are cultivated for crops such as kales, tomatoes, cabbages, carrots, onions, avocadoes and coffee (Karuku *et al*., 2012).

## 4.2 Data Collection Approach

### 4.2.1 Experimental Set-up

Field experiments were conducted to collect draft force datasets. Draft datasets were recorded using a data logging station consisting of an MSI 7300 digital dynamometer communicating

wirelessly with a MSI8000 remote display that streamed data directly into a laptop computer via the serial port.


**Plate 4.1: Field Data logging station Setup**

Plate 4.2 show close-up images of the dynamometer and the remote display;


MSI 7300 Dynalink 2 MSI 8000 Remote Display

**Plate 4.2: Digital Dynamometer Components**

Since the dynamometer could not be connected directly at the three point hitch of the towed tool carriage, it was attached as shown in Figure 4.3. The tillage tines to be tested were attached to the tool carriage which was attached to the three point hitch of the towed tractor (i.e. gear lever in neutral position); the dynamometer was attached between the rear towed tractor and the front towing tractor via steel shackles. For convenience and safety during experimental runs; the digital dynamometer streamed data remotely into the stationary data logging station that was manned by a data collection assistant. A single experimental run yielded several data points; the number of data points was dependent on the stability of the

dynamometer during the run, the draft for a particular run was thus taken as average of the recorded data points for the run.

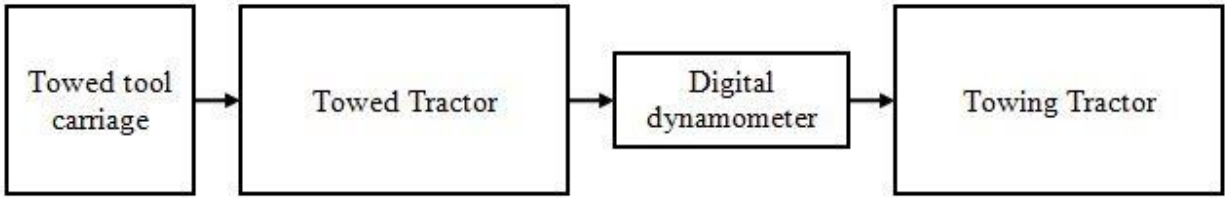


**Figure 4.2: The experimental set-up**

At the start of the experiments, a dry-run of the system described in Figure 4.3 was executed with the tillage tines disengaged to establish the rolling resistance of the rear towed tractor and the towed tool carriage, this value was subtracted from the draft data at the end of the experiments to establish the draft requirement as a result of the tillage tine alone.

**Plate 4.3: A trial run with the dynamometer anchored between the tractors**

**Plate 4.4: Tool carriage with the 60$^{o}$ ripper attached**

### 4.2.2 Experimental Design

The Factorial Completely Randomized Block design was the statistical technique used to investigate the effects of the forward speed and rake angle on the draft force requirement of a 5cm wide ripper tine. This experimental design helps the researcher study more than one independent variables that may have a combined effect on a particular dependent variable. Randomization eliminates bias while blocking enables uniform response to reduce experimental error.

Field investigations studied the rake angle in four levels (30$^{o}$, 45$^{o}$, 60$^{o}$ and 75$^{o}$), tillage depth in three levels (15, 25 and 40 cm) and forward speed in 2 levels (3 and 5 km/hr.); each treatment was replicated four times (once per block) to yield a total of 96 treatments for the experiment.

The experiment was conducted at the University Field Station farms on an experimental plot of 50 meters by 20 meters, this plot was sub-divided into four subplots of equal size each measuring 25 meters by 10 meters; an allowance area of 5 meters in length was left at the start and end of each sub-plot for staging, practice and turning.

The four experimental blocks were selected to eliminate variation due to distance and slope along the experimental farm. Randomization was carried out separately for each rake angle; this involved writing down the treatments for each rake angle on pieces of paper, putting

them in a basket and then drawing them one by one without replacement from the basket and then executing the treatments in the order they were drawn from the basket; this was done separately for each of the four rake angles.

### 4.2.3 Soil data-sets collected

Soil samples were taken from the field for various types of analyses in the soils laboratory; the soil was sampled systematically in accordance to the technique demonstrated in Figure 4.4. Sampling was done at three levels (0 – 15cm, 15 – 25cm, 25 – 40cm) making a total of 12 sampling points and 36 soil samples.

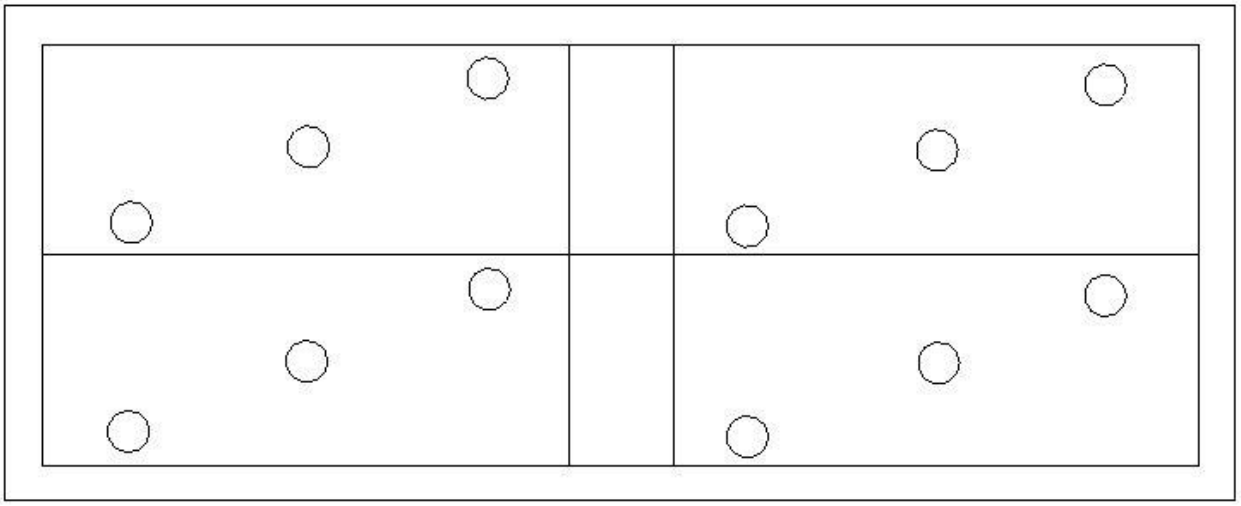

**Figure 4.3: Soil sampling technique adopted**

The sampled soils were analyzed in the soils laboratory for the following properties;

**a) Moisture Content**

The moisture content of the soil was established using the **gravimetric method**. Soil sampled for moisture content analysis was taken just before a run and kept in moisture bags to prevent drying. The soil was weighed, oven dried at 105$^{o}$C for 72hrs and then re-weighed. The moisture content was obtained as the ratio of the difference in weight between the original and the oven dried soil to the original weight.

**b) Wet Bulk density**

The wet bulk density of the soil was measured using the **core cutter method**. This involved hammering a core ring of known dimensions into the spot where the bulk density was to be established; once filled with soil, the ends of the ring were trimmed off using a straight edge.

The weight and moisture content of the contained soil was established and the bulk density was obtained as the ratio of the weight of the wet soil to the internal volume of the core ring.

**c) Particle size analysis**

Particle size analysis was carried out using the standard **sieve analysis method** recommended by ASTM to establish the distribution of the grain sizes. The soil was then classified based on the average clay, sand and silt content.

**d) Particle Shape Characterization**

Soil particle shape is an important input factor for computer simulation using EDEM Academic™; soil samples from the sieve analysis procedure were taken to the soils laboratory at the Department of LARMAT for shape characterization.

The process involved placing a scoop of soil from each of the sieve under a lit microscope and zooming in to obtain a sharp view of the particle silhouette; a snapshot was then captured using a high resolution digital camera.

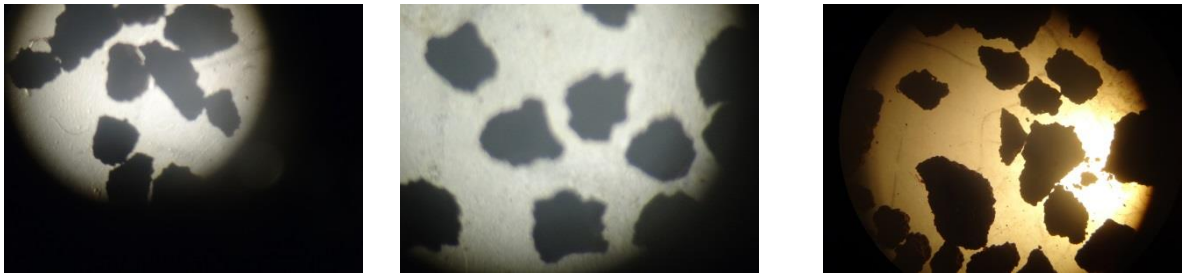

**Plate 4.5: Soil particle shapes observed under the microscope**

**e) Triaxial test parameters (Cohesion and Angle of Internal Friction)**

The **triaxial test** was carried out with the triaxial apparatus available at the soils laboratory at Upper Kabete campus to establish the shear strength parameters of the soil (i.e. cohesion and the angle of internal friction). Soil sampling for the triaxial test was done using a special core ring; a rubber membrane was then fitted around the samples which were then placed inside the triaxial cell and loaded to failure with a pneumatic confining pressure applied.

**f) Cone Index**

The cone index was obtained using a pocket penetrometer of conforming to ASAE standards of $30^{o}$ cone angle and a diameter of 12.83 mm. The test involved twisting the penetrometer on a soil surface while applying a penetration load by hand until the vane of the penetrometer sheared the soil; the reading of the index was obtained from the graph attached to the devise.

### g) Angle of Repose Test

This test involved pouring the air-dried soil sample in a funnel and letting it flow at the narrow end of the funnel unimpeded on to a flat surface until a conical lump is formed; the angle the material made with the surface is the angle of repose.

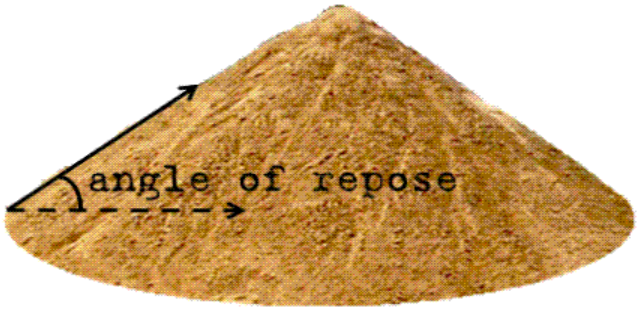


**Figure 4.4: Angle of repose. Source (SERC, 2014)**

### 4.2.4 Computer Simulation

The EDEM Academic™ software from DEM Solutions Limited was applied to solve for the draft forces to ripping using various tool geometries. The model was calibrated by simulating the angle of repose test; the model parameters that gave a behavior similar to the angle of repose were selected as the suitable calibration parameters for the model.

Soil particle shapes were characterized in the soils laboratory were modeled in EDEM Academic™ as a clump of spheres as described in Figure 4.5; the process involved combining three spheres of a similar diameter to form the target soil particle shape of a given diameter;

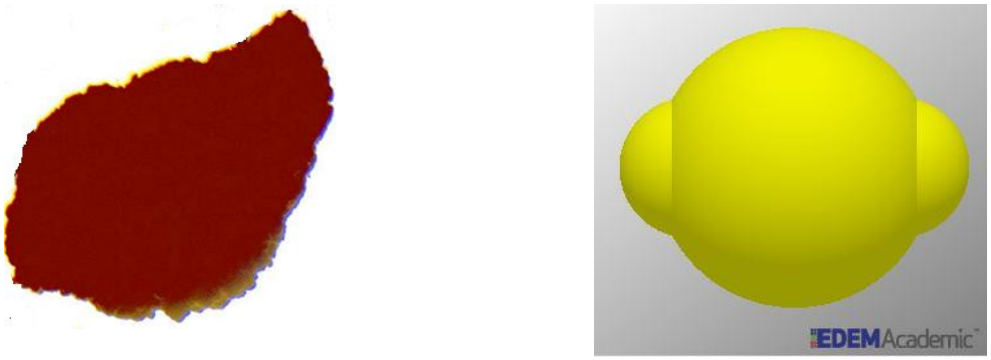


Soil Particle Shape Remodeled Particle Shape in EDEM Academic™

**Figure 4.5: Soil particle shape remodeling**

Three types of geometries i.e. the Virtual Box, Tillage Tine Models and a Particle Factory were created as follows;

1. **Virtual Box**

The virtual box is an experimental soil bin created in the EDEM Academic™ environment to hold the particles generated to simulate a mass of soil in an experimental farm. The virtual box created was of dimensions 400mm length, 200mm width by 500mm height.

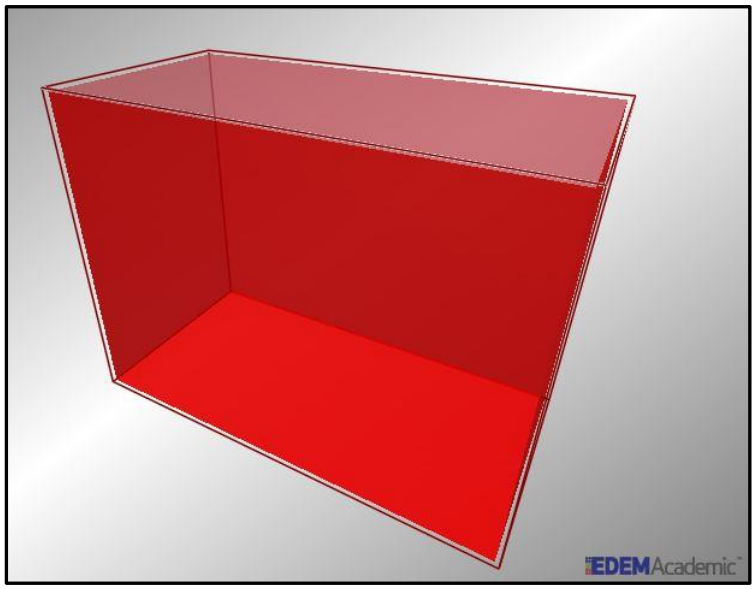


**Figure 4.6: Empty Virtual Box**

2. **Tillage Tine Models**

The following tillage tines were used in the field experiments;

**Figure 4.7: Ripper tines used ($75^o$, $60^o$, $45^o$ and $30^o$ rake angles respectively)**

The tillage tines were modeled in AutoCAD Mechanical 2015 and saved in a .stp file format. The AutoCAD models of the tines are as shown in Figure 4.8;

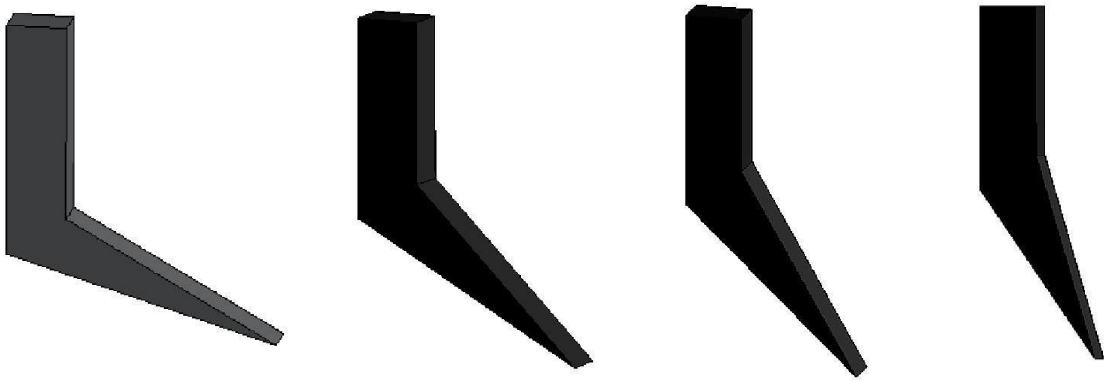

30$^{o}$ Ripper Tine 45$^{o}$ Ripper Tine 60$^{o}$ Ripper Tine 75$^{o}$ Ripper Tine

**Figure 4.8: Ripper Tines Remodeled in AutoCAD**

The created tine models were imported into EDEM Academic™ via the geometry import tool repositioned and aligned along the longitudinal axis of the virtual box.

### 3. Particle Factory Plate

A rectangular plate of 400 mm by 200mm was created in EDEM Academic™ to generate particles and fill them into the virtual Box.

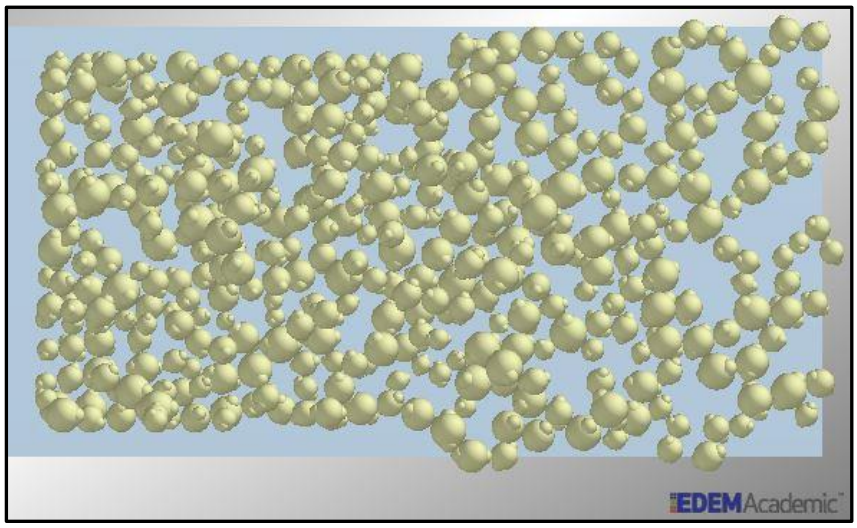


**Figure 4.9: Particles dropping from the Particle Factory®**

The EDEM Academic™ was initiated and the units set to S.I (International System of Units); the simulation then proceeded in the manner described in Sections 3.3.2, 3.3.3 and 3.3.4. The results of the simulation process (i.e. Draft force data) were then exported in a .csv format for analysis in Microsoft Excel and SPSS.

### 4.2.5 Statistical Analysis

#### *4.2.5.1 Elimination of Outliers*

The digital dynamometer registered several datasets and various points during a single experimental run; the number of data points depended on the stability of the tool carriage (i.e. freedom from vibrations) during the run; as such, some of the data points recorded were way below or above the mean of the recorded data stream.

To eliminate the outliers in the measured draft datasets, the **median of the data-streams** was used; these data sets were thus representative of the actual draft data.

#### *4.2.5.2 Investigation of the Normality of the Measured and Predicted draft datasets*

ANOVA, the t-test and regression analysis assume that the datasets being subjected to the tests exhibit a normal distribution; it was therefore imperative to check the normality of the draft datasets before subjecting them to statistical analysis. Normality and other assumptions should be considered because when these assumptions do not hold, it is impossible to draw accurate and reliable inferences about the study.

The cleaned draft dataset were subjected to the One Sample Kolmogorov-Smirnov Test in SPSS to check their distribution; the null hypothesis tested was that the datasets were normally distributed. The One Sample Kolmogorov-Smirnov Test, the null hypothesis is accepted when the p-value is greater than 0.05.

#### *4.2.5.3 Analysis of Variance*

The Analysis of Variance (ANOVA) is a statistical technique of comparing different sources of variance within a data set with the aim of determining if significant differences exist between two or more groups.

The statistic for ANOVA is the F ratio; if the variance amongst the sample mean is greater than the variance due to error, the F-Statistic is greater than one. In ANOVA, a test is conducted to see whether the F-Statistic is greater than one or not and this forms the null hypothesis.

$$\text{F Statistic} = \frac{\text{variance among sample means}}{\text{variance within samples}} \tag{4.1}$$

The ANOVA was applied to test whether the treatments (i.e. differences in blocks, rake angles, ripping depths and operating speeds) had an effect on the specific draft. The null

hypothesis tested was that the treatments had an effect on the specific draft. ANOVA of the specific draft data as a result of the treatment effects means was conducted in SPSS.

#### *4.2.5.4 The Student t-test*

The student t-test assesses whether the means of two groups are statistically similar or different from each other; it renders itself useful whenever two means of two samples from two different populations are being compared.

The student t-test was applied to test whether the mean of the measured specific draft was significantly similar or different from the mean of the predicted specific draft. The null hypothesis tested was that the two means where similar. The t-test for the similarity of the means was conducted using SPSS.

$$\text{t-value} = \frac{\text{Signal}}{\text{Noise}} = \frac{\text{Difference between group means}}{\text{Variability of groups}} \tag{4.2}$$

#### *4.2.5.5 Linear Regression*

Linear regression is an approach for evaluating the relationship between a dependent variable and one or more independent variables. The most common form of linear regression is least squares fitting in which the line of best – fit that minimizes the sum of squares of residuals is found; linear regression also provides the coefficient of determination ($R^2$) and coefficient of correlation (r) that indicate quality of fit.

$$r = R^{1/2} = 1 - \frac{\text{Residual Sum of Squares}}{\text{Total Sum of Squares}} \tag{4.3}$$

# CHAPTER FIVE: RESULTS AND DISCUSSIONS

## 5.1 Preamble

This chapter presents the findings and interpretation of the various datasets obtained during the research. The soil characteristics of the study site are presented herein; the draft data from experiments and the statistical treatments are also provided. Numerical simulation with EDEM Academic™ is explained in details and the predicted draft datasets presented. Statistical analysis and comparison of the measured and predicted datasets are also presented; an evaluation of the effect of the rake angle, tillage depth and operating speed was conducted and has been presented.

The detailed field data and the predicted data are provided in Appendix B.

## 5.2 Experimental Site Soil Characteristics

Soil sample analysis was conducted in the soils laboratory, Department of Environmental and Biosystems Engineering at Upper Kabete. The following soil properties were obtained;

**Table 5.1: Site soil characteristics**

| No | Parameter | Average Value |
|---|---|---|
| 1. | Dry Density | 1818 kg/$m^3$ |
| 2. | Wet Bulk Density | 1322.5 kg/$m^3$ |
| 3. | Angle of Repose (Experimental) | 34$^o$ |
| 4. | Angle of Repose (Simulation) | 33.6$^o$ |
| 5. | Moisture Content | 19% |
| 6. | Cone Index (kPa) | 220.56 |
| 7. | Insitu Cohesion (kPa) | 3 |
| 8. | Insitu Angle of Internal friction (degrees) | 10 |
| 9. | Soil Classification | Sandy Clay<br>(54% Sand, 35%Clay, 11%Silt) |

## 5.3 Experimental data analysis

Experimental runs for the various treatments yielded the following data;

### 5.3.1 Rolling Resistance

The rolling resistance of the rear tractor and tool carriage was recorded using the dynamometer at the inception of field investigations by drawing the rear systems without

engaging the tool to the soil. The following data series was logged by the dynamometer into the laptop;

**Table 5.2: Rolling Resistance**

| No. | Rolling Resistance (kN) |
|---|---|
| 1 | 1.21 |
| 2 | 1.07 |
| 3 | 1.00 |
| 4 | 1.16 |
| 5 | 1.23 |
| 6 | 1.00 |
| 7 | 1.03 |
| **Median** | **1.07** |

Since the data was observed to contain outliers (i.e. 1.21kN and 1.23kN), the median of the dataset of **1.07kN** was taken to be the rolling resistance for the system. This value was then subtracted from the gross draft force to obtain the net draft force.

### 5.3.2 Statistical Evaluation of the Normality of Measured Draft Data

The value of the rolling resistance obtained above was subtracted from all the draft values to obtain the net draft. The draft values were then divided by the width of each tool (i.e. 5cm) to obtain the specific draft.

The measured specific draft data was tested for normality by employing the One Sample Kolmogorov-Smirnov Test in SPSS; the following hypothesis was tested;

$H_o$: The data sets are normally distributed

$H_1$: The data sets are not normally distributed

**Table 5.3: One-Sample Kolmogorov-Smirnov Test for the Measured Draft Data**

| | | Block 1 | Block 2 | Block 3 | Block 4 |
|---|---|---|---|---|---|
| N | | 24 | 24 | 24 | 24 |
| Normal Parameters[a,b] | Mean | 1.1192 | 1.1392 | 1.1904 | 1.2212 |
| | Std. Deviation | 0.81692 | 0.82774 | 0.83387 | 0.94309 |
| Most Extreme Differences | Absolute | 0.249 | 0.238 | 0.238 | 0.264 |
| | Positive | 0.249 | 0.238 | 0.238 | 0.264 |
| | Negative | -0.125 | -0.118 | -0.130 | -0.142 |
| Kolmogorov-Smirnov Z | | 1.218 | 1.167 | 1.167 | 1.291 |
| Asymp. Sig. (2-tailed) | | 0.103 | 0.131 | 0.131 | 0.071 |

a. Test distribution is Normal.

b. Calculated from data.

The p-values for all the replications were all found to be greater than 0.05 at the 95% level of confidence; the null hypothesis that the data sets were normally distributed was accepted.

### 5.3.3 Investigation of the effect of Parameters on Measured Draft Data

The measured specific draft datasets were rearranged as shown in Appendix B for ANOVA in SPSS with specific draft as the dependent variable and block, speed, rake angle and depth as the factors. The following hypothesis test was conducted;

$H_o : \mu_1 = \mu_2$
$H_1 : \mu_1 \neq \mu_2$

**Table 5.4: ANOVA for the Measured Draft data**

| Dependent Variable: Exp_Draft | | | | | |
|---|---|---|---|---|---|
| **Source** | **Type III Sum of Squares** | **df** | **Mean Square** | **F** | **Sig.** |
| Model | 197.962[a] | 39 | 5.076 | 477.339 | 0.000 |
| Block | 0.157 | 3 | 0.052 | 4.930 | 0.004 |
| Speed | 1.247 | 1 | 1.247 | 117.239 | 0.000 |
| Rake | 4.263 | 3 | 1.421 | 133.635 | 0.000 |
| Depth | 56.774 | 2 | 28.387 | 2669.513 | 0.000 |
| Block * Depth | 0.177 | 6 | 0.029 | 2.771 | 0.020 |
| Block * Rake | 0.011 | 9 | 0.001 | 0.112 | 0.999 |
| Block * Speed | 0.092 | 3 | 0.031 | 2.899 | 0.043 |
| Rake * Depth | 2.385 | 6 | 0.398 | 37.386 | 0.000 |
| Speed * Depth | 1.950 | 2 | 0.975 | 91.666 | 0.000 |
| Speed * Rake | 0.052 | 3 | 0.017 | 1.633 | 0.192 |
| Error | 0.606 | 57 | 0.011 | | |
| Total | 198.568 | 96 | | | |
| a. R Squared = 0.997 (Adjusted R Squared = 0 .995) | | | | | |

The p-values for the main effects (i.e. Block, Speed, Rake Angle and Depth) were all found to be less than 0.05 with 95% of confidence; the null hypothesis was thus rejected in favor of the alternative. It was thus concluded that the main effects were significantly influential to the specific draft force. Further, the interaction between Block and speed, Rake Angle and Depth, Block and depth and Speed and depth were also found to influence the specific draft force.

### 5.4 Numerical Simulation

EDEM Academic™ version 2.7.0 was employed to conduct numerical simulation of the tillage process. The computer used was a Toshiba Qosmio® Laptop with an i7 processor (2.64 Ghz Quad core), RAM of 8GB, storage space of 1TB and a 64-bit Windows 7 Operating System. The simulation proceeded as follows;

### 5.4.1 Global settings

The units of measurement were set to SI to be used throughout the simulation; the following global settings were made in the main window of EDEM Academic™;

**Table 5.5: Global Settings in EDEM Academic™**

| Property | Units | Value |
|---|---|---|
| Work Function | eV | $0$ |
| Gravity | $m/s^2$ | $-9.81$ |
| Poisson's Ratio of Steel | No units | $0.3$ |
| Shear Modulus of Steel | Pascals | $7 \times 10^{10}$ |
| Density of Steel | $kg/m^3$ | $7850$ |
| Poisson's Ratio of Soil | No units | $0.25$ |
| Shear Modulus of Soil | Pascals | $1 \times 10^{7}$ |
| Density of Soil | $kg/m^3$ | $1818$ |

The properties of the re-created soil particles were automatically calculated in EDEM Academic™ to be as follows;

**Table 5.6: EDEM Academic™ particle properties**

| Property | Value |
|---|---|
| Base Particle Radius | 4mm |
| Contact Radius | 4mm |
| Calculated Particle Mass | 0.000515066 kg |
| Calculated Particle Volume | 2.83314e-07 $m^3$ |
| Particle Material | Soil |

### 5.4.2 Particle Factory

Particle factories are used to define where, when and how particles appear in a simulation. A dynamic factory type was specified in EDEM to enable the creation of particles as the simulation continued. The following settings were made to the factory;

**Table 5.7: Particle Factory® settings**

| Parameter | Setting |
|---|---|
| Factory Type | Dynamic |
| Number or mass of particles | Unlimited in Number |
| Generation rate | 4000 Particles/second |
| Start time | 0 Seconds |
| Max attempts to place particle | 20 |

The following initial conditions were also specified for the particle factory in EDEM Academic™;

**Table 5.8: Particle creation settings**

| Parameter | Setting |
|---|---|
| Section | Particle Factory Plate |
| Type | Fixed particle type |
| Size | Log-normal distribution<br>Mean: 0.7769, Standard Deviation: 1.82261 |
| Scale Size by | Radius |
| Position | Positioned randomly |
| Velocity | Fixed velocity (V= -20m/s) |
| Orientation | Random orientation |

### 5.4.3 EDEM Simulator® Settings

The EDEM Simulator® was configured to the following settings;

**Table 5.9: EDEM Academic Simulator Settings**

| Parameter | Setting |
|---|---|
| Fixed Time Step | 20% of the Raleigh time step |
| Total Simulation Time | 15 seconds |
| Target Save Interval | 0.1 seconds |
| Simulator Grid Cell Size | 6 R-Min |
| Approximate number of Cells | 53,568 |
| Number of Cores | 4 |

### 5.4.4 EDEM Model Calibration and Full Scale Simulation Runs

Calibrating an EDEM Academic™ model involved adjusting the model parameters until the model produced results that matched a physical test after a batch simulation operation; in this case, the angle of repose test was the physical test used to calibrate the model.

The model parameters adjusted included Surface Energy value for the Hertz-Mindlin with JKR contact model (5, 10, 15, and 20 J/m$^2$), Coefficient of Static Friction (0.2, 0.4, and 0.6), Coefficient of Rolling Friction (0.06 and 0.12) and the Coefficient of Restitution (0.1, 0.2, 0.3, and 0.4).

A total of 94 simulations in batch mode representing 94 different and exclusive combinations of the above parameters were executed; the angles of repose were measured in EDEM Analyst® using the protractor tool; the parameter combination that gave an angle of repose similar to the physical test is given in Table 5.10;

**Table 5.10: Soil *en-masse* calibration parameter settings**

| **Parameter** | **Value** |
|---|---|
| Filename | JKR-5J-0.2CR-0.4SF-0.06RF.dem |
| JKR Surface Energy (J/m$^2$) | 5 |
| Coefficient of Restitution | 0.2 |
| Coefficient of Static Friction | 0.4 |
| Coefficient of Rolling Friction | 0.06 |
| Angle of Repose (EDEM Academic™) | 33.6$^o$ |
| Angle of Repose (Physical Test) | 34$^o$ |

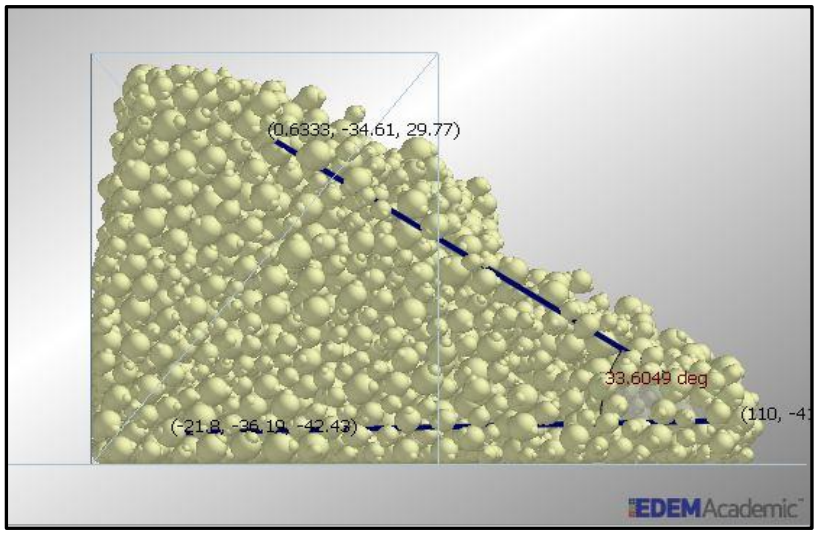


**Figure 5.1: Slumped soil mass in EDEM Academic™ showing the angle of repose**

The angle of repose as shown in Figure 5.1 was measured using a protractor tool built in EDEM Analyst® for that particular purpose. The calibration parameters obtained were then used to conduct the full scale simulation runs. The complete list of the angles of repose determined for the different calibration settings are provided in Appendix C.

Figure 5.2 shows a modeled ripper tine aligned along the longitudinal axis of the Virtual Box ready for a trial run.

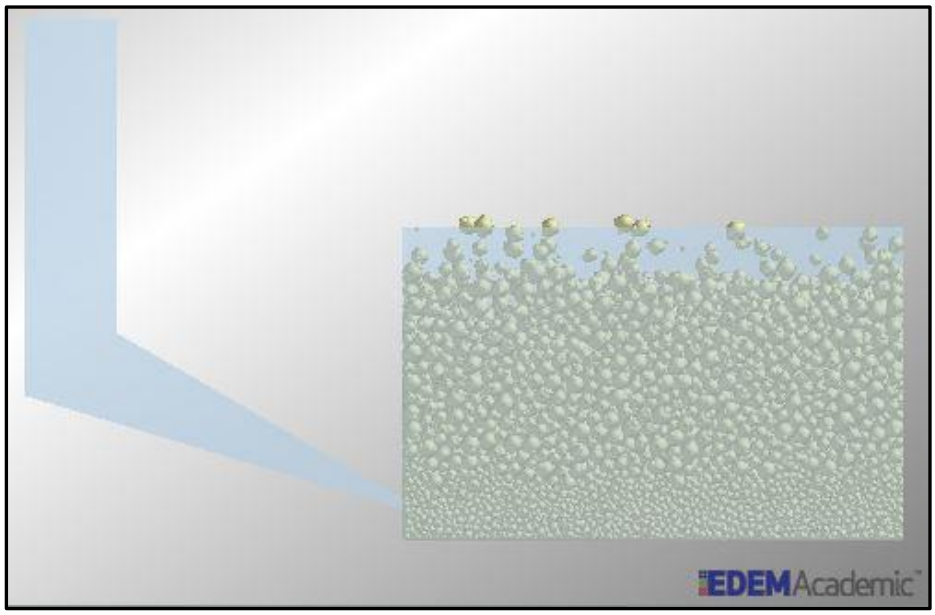


**Figure 5.2: Tool Aligned Along the virtual box axis ready for a simulation run**

The results of the simulation runs extracted from the EDEM Analyst® by creating queries that displayed the horizontal forces on the ripper tine face perpendicular to the direction of travel. The extracted datasets were exported from the EDEM Analyst® to Microsoft Excel in a comma-separated (.csv) format for cleaning and analysis. The cleaned predicted specific draft force datasets are provided in Appendix B.

### 5.4.5 Statistical Evaluation of the Normality of Predicted Draft Data

The predicted draft data was tested for normality by employing the One Sample Kolmogorov-Smirnov Test in SPSS; the following hypothesis was tested;

$H_o$: The data sets are normally distributed

$H_1$: The data sets are not normally distributed

**Table 5.11: One-Sample Kolmogorov-Smirnov Test for the Predicted Draft Data**

| | | |
|---|---|---|
| N | | 24 |
| Normal Parameters[a,b] | Mean | 1.1667 |
| | Std. Deviation | 0.83622 |
| Most Extreme Differences | Absolute | 0.255 |
| | Positive | 0.255 |
| | Negative | -0.124 |
| Kolmogorov-Smirnov Z | | 1.249 |
| Asymp. Sig. (2-tailed) | | 0.088 |
| a. Test distribution is Normal. | | |
| b. Calculated from data. | | |

The p-value for the predicted datasets was found to be greater than 0.05 at the 95% level of confidence; the null hypothesis that the data sets were normally distributed was accepted.

### 5.4.6 Investigation of the effect of Parameters on Predicted Draft Data

The predicted draft datasets were rearranged as shown in Appendix B for Univariate Analysis in SPSS with specific draft as the dependent variable and block, speed, rake angle and depth as the factors. The following hypothesis test was conducted;

$H_o : \mu_1 = \mu_2$
$H_1 : \mu_1 \neq \mu_2$

**Table 5.12: ANOVA for the Predicted Draft data**

| Dependent Variable: EDEM_Draft | | | | | |
|---|---|---|---|---|---|
| **Source** | **Type III Sum of Squares** | **df** | **Mean Square** | **F** | **Sig.** |
| Corrected Model | 64.531[a] | 38 | 1.698 | 1062.916 | 0.000 |
| Intercept | 129.456 | 1 | 129.456 | 81028.557 | 0.000 |
| Block | 0.000 | 3 | 0.000 | 0.000 | 1.000 |
| Speed | 1.101 | 1 | 1.101 | 689.018 | 0.000 |
| Rake | 4.108 | 3 | 1.369 | 857.069 | 0.000 |
| Depth | 55.091 | 2 | 27.545 | 17241.081 | 0.000 |
| Block * Depth | 0.000 | 6 | 0.000 | 0.000 | 1.000 |
| Block * Rake | 0.000 | 9 | 0.000 | 0.000 | 1.000 |
| Block * Speed | 0.000 | 3 | 0.000 | 0.000 | 1.000 |
| Rake * Depth | 2.513 | 6 | 0.419 | 262.147 | 0.000 |
| Speed * Depth | 1.672 | 2 | 0.836 | 523.307 | 0.000 |
| Speed * Rake | 0.046 | 3 | 0.015 | 9.636 | 0.000 |
| Error | 0.091 | 57 | 0.002 | | |
| Total | 194.078 | 96 | | | |
| Corrected Total | 64.622 | 95 | | | |
| a. R Squared = 0.999 (Adjusted R Squared = 0.998) | | | | | |

The p-values for the main effects (i.e. Speed, Rake Angle and Depth) were all found to be less than 0.05 with 95% of confidence; the null hypothesis was thus rejected in favor of the alternative. It can thus be concluded that the main effects were significantly influential to the draft force. Further, the interaction between Rake Angle and Depth, Speed and Rake Angle and Speed and depth were also found to influence the draft force.

### 5.5 Statistical Comparison of the Measured and Predicted Datasets

The experimental draft dataset and the EDEM Academic™ draft dataset were subjected to a paired samples t-test in SPSS to compare their means; the following hypotheses were tested;

$$H_o : \mu_1 = \mu_2$$
$$H_1 : \mu_1 \neq \mu_2$$

The results are as shown in Table 5.13;

**Table 5.13: Paired Samples t - Test for the Draft Data**

| | Paired Differences | | | | | t | df | Sig. (2-tailed) |
|---|---|---|---|---|---|---|---|---|
| | Mean | Std. Dev | Std. Error Mean | 95% Confidence Interval of the Difference | | | | |
| | | | | Lower | Upper | | | |
| Exp_Draft - EDEM_Draft | 0.0063 | 0.0998 | 0.01019 | -0.014 | 0.02648 | 0.613 | 95 | 0.541 |

The p-value is greater than 0.05 (i.e. 0.541 > 0.05), the null hypothesis is thus accepted; this implies that the there is strong evidence to indicate that the experimental draft dataset is significantly similar to the EDEM Academic™ draft dataset; the interpretation is that EDEM Academic™ accurately modelled the tillage process.

Linear regression was conducted in SPSS to investigate the degree of fit of the experimental datasets to the EDEM Academic™ dataset; results indicated an extremely good fit with a coefficient of determination ($R^2$) of 0.986. Figure 5.3 also shows the 95% confidence level line bounds; most of the data points line within the 95% confidence interval further confirming the excellent degree of fit between the two datasets.

The line of fit is linear with a slope of one and passing through the origin of the graph; this indicates that the two datasets are almost similar showing that the developed model accurately reflected the true ripping conditions and that the simulation model was of high fidelity. Figure 5.3 provides the line of fit with the two lines on either side of the line of fit defining the 95% confidence bounds; it can be observed that most of the measured/ observed data points fall within the 95% confidence interval.

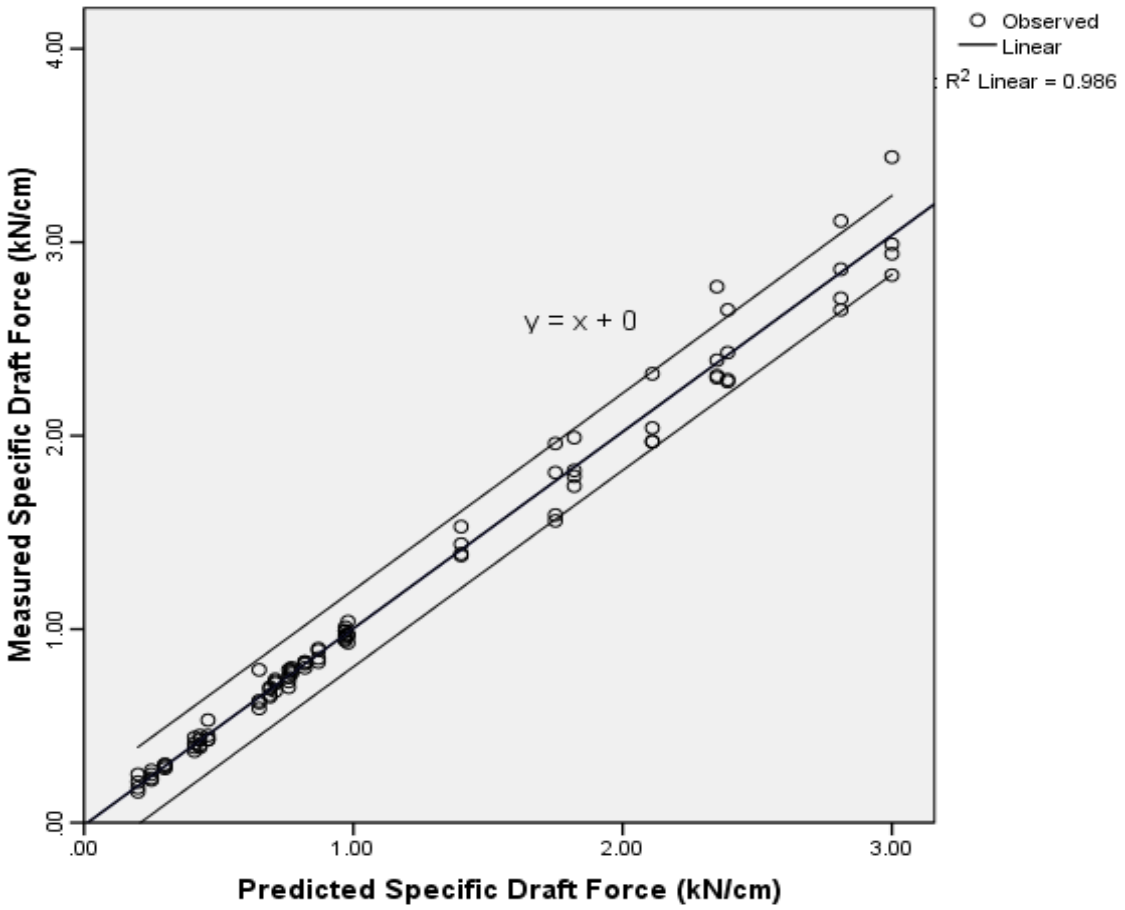


**Figure 5.3: Linear regression between Measured and Predicted Specific Draft Force**

### 5.6 The Influence of Tool and Operational Parameters on the Draft Force

Graphical representation of the effects of the factors on the specific draft is as shown in the Figures that follow;

#### 5.6.1 Effect of the Rake Angle

The draft force reduced from a rake angle of $30^o$ to attain a minimum at an angle of $45^o$ then increased exponentially to the rake angle of $75^o$ as described in Figure 5.4. This finding agreed with the observations of Tong and Moayad (2006) and Maswaure (1995) who recommended that for minimizing the draft forces, the tool rake angles must be set to between $30^o$ and $60^o$.

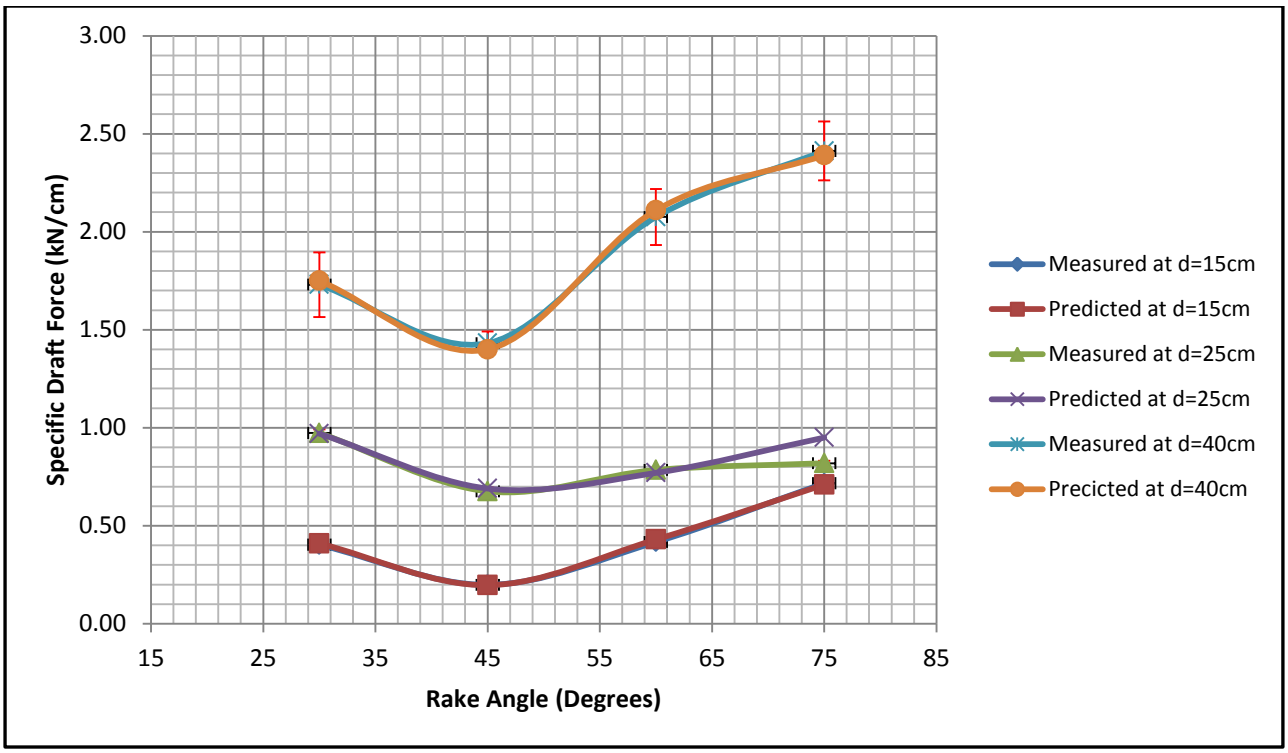


**Figure 5.4: Specific Draft Force against Rake Angle at an Operating Speed of 3kph**

Table 5.14 gives the equations of best fit and the coefficients of determination to the above plots at the speed of 3kph; the equations are cubic in nature with a coefficient of determination ($R^2$) of 1.00 indicating an exact fit to the plots.

**Table 5.14: Equations of Best Fit at Operating Speed of 3kph**

| Speed (Kph) | Depth (Cm) | Equation of Best Fit | Coefficient of Determination ($R^2$) |
|---|---|---|---|
| 3 | 15 | $y = -2E\text{-}05x^3 + 0.0037x^2 - 0.2038x + 3.77$ | 1.00 |
| 3 | 25 | $y = -1E\text{-}05x^3 + 0.0025x^2 - 0.1538x + 3.65$ | 1.00 |
| 3 | 40 | $y = -7E\text{-}05x^3 + 0.0123x^2 - 0.6304x + 11.59$ | 1.00 |

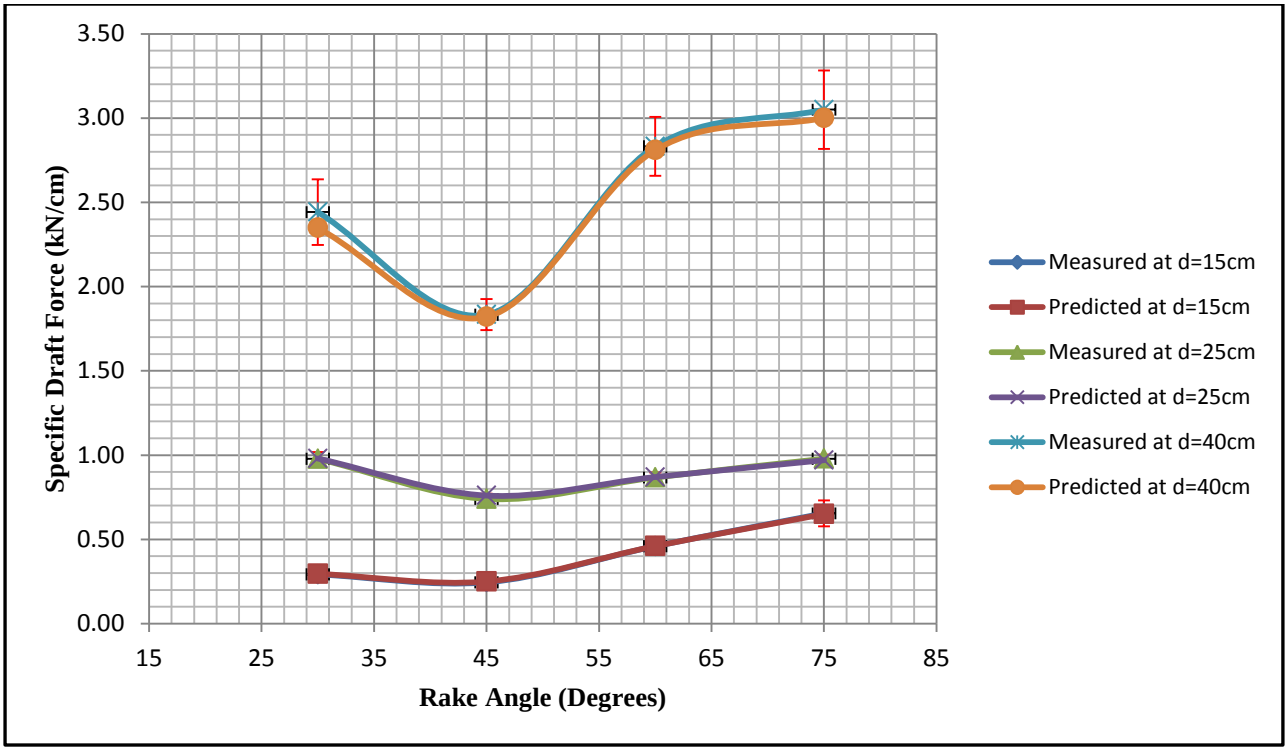


**Figure 5.5: Specific Draft Force Against Rake Angle at an Operating Speed of 3kph**

Table 5.15 gives the equations of best fit and the coefficients of determination to the above plots at the speed of 5kph; the equations are cubic in nature with a coefficient of determination ($R^2$) of 1.00 indicating an exact fit to the plots.

**Table 5.15: Equations of Best Fit at Operating Speed of 5kph**

| Speed (Kph) | Depth (Cm) | Equation of Best Fit | Coefficient of Determination ($R^2$) |
|---|---|---|---|
| 5 | 15 | $y = -0.0001x^3 + 0.0188x^2 - 0.9578x + 17.23$ | 1.00 |
| 5 | 25 | $y = -2E\text{-}05x^3 + 0.003x^2 - 0.1679x + 3.77$ | 1.00 |
| 5 | 40 | $y = -0.0001x^3 + 0.0188x^2 - 0.9578x + 17.23$ | 1.00 |

The equations of best fit at both speed levels (3 and 5kph), were cubic in nature displaying a local minimum at a rake angle of $45^o$ and a local maximum at the rake angle of $75^o$.

### 5.6.2 Effect of Tillage Depth

Sahu & Raheman (2006) emphasized the significance of the working depth in any tillage operation. In their studies, they discovered that the draft values of all reference tillage tools and hence, scale-model/prototype implements were found to be primarily dependent on depth of operation.

Due to varying field conditions, the following tillage depths were attained in this study;

**Table 5.16: Tillage depths attained during field investigations**

| Tillage Tine (degrees) | Level (cm) | Tillage Depth Attained (cm) |
|---|---|---|
| 30 | 0 - 15 | 15 |
| | 15 - 25 | 24 |
| | 25 - 40 | 38 |
| 45 | 0 - 15 | 15 |
| | 15 - 25 | 24 |
| | 25 - 40 | 38 |
| 60 | 0 - 15 | 15 |
| | 15 - 25 | 20 |
| | 25 - 40 | 40 |
| 75 | 0 - 15 | 15 |
| | 15 - 25 | 20 |
| | 25 - 40 | 40 |

The draft increased in a near linear manner with increase in the tillage depth as described by the equations of a straight line inside the plots; this indicated that the draft force was directly proportional to the tillage depth. The measured specific draft values at the two levels of speed converged at ripping depths less than 25cm; this could be due to the presence of a loose layer of soil above the 25cm depth that gave similar draft force values regardless of the operating speed; the difference was however more pronounced for the predicted specific draft values.

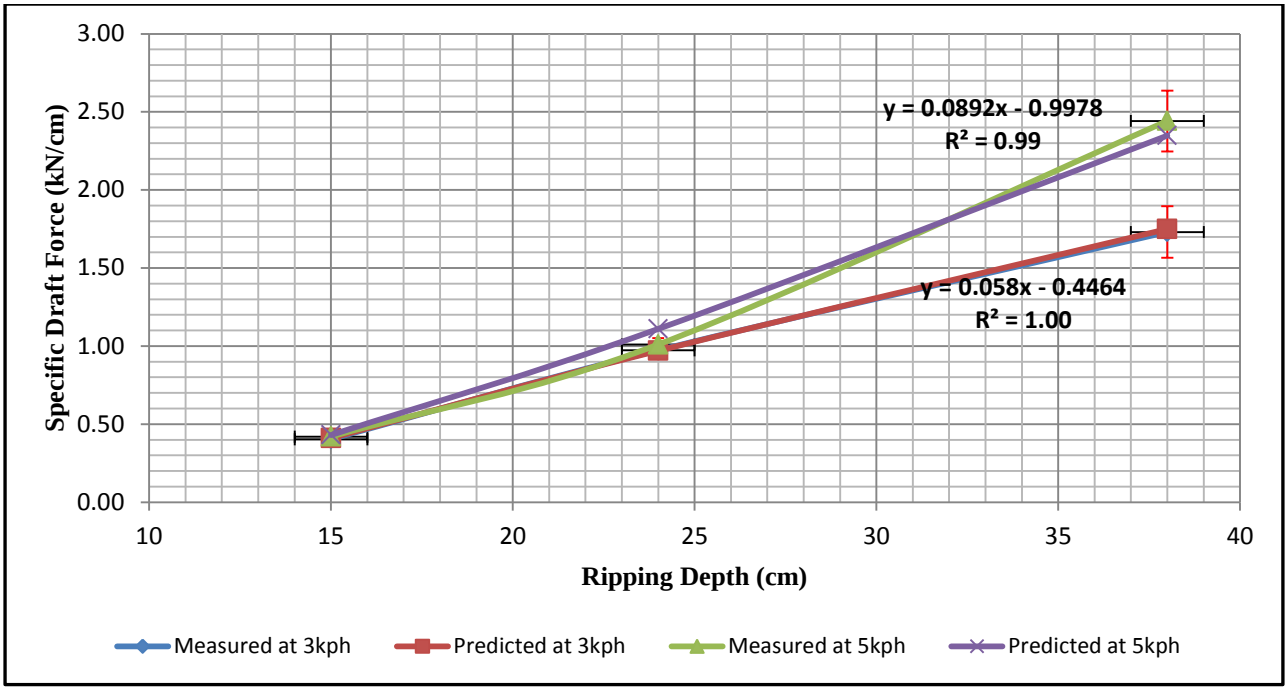


**Figure 5.6: Specific Draft Force against Ripping Depth at a Rake Angle of 30$^{o}$**

At the rake angle of 30 degrees, this study found both the measured and predicted specific draft to increase in a linear manner with the ripping depth. Increasing the ripping depth from 15cm to about 40cm resulted to an increase in the specific draft by 1.33 kN/cm at the speed of 3kph and by 2.15 kN/cm at the speed of 5kph.

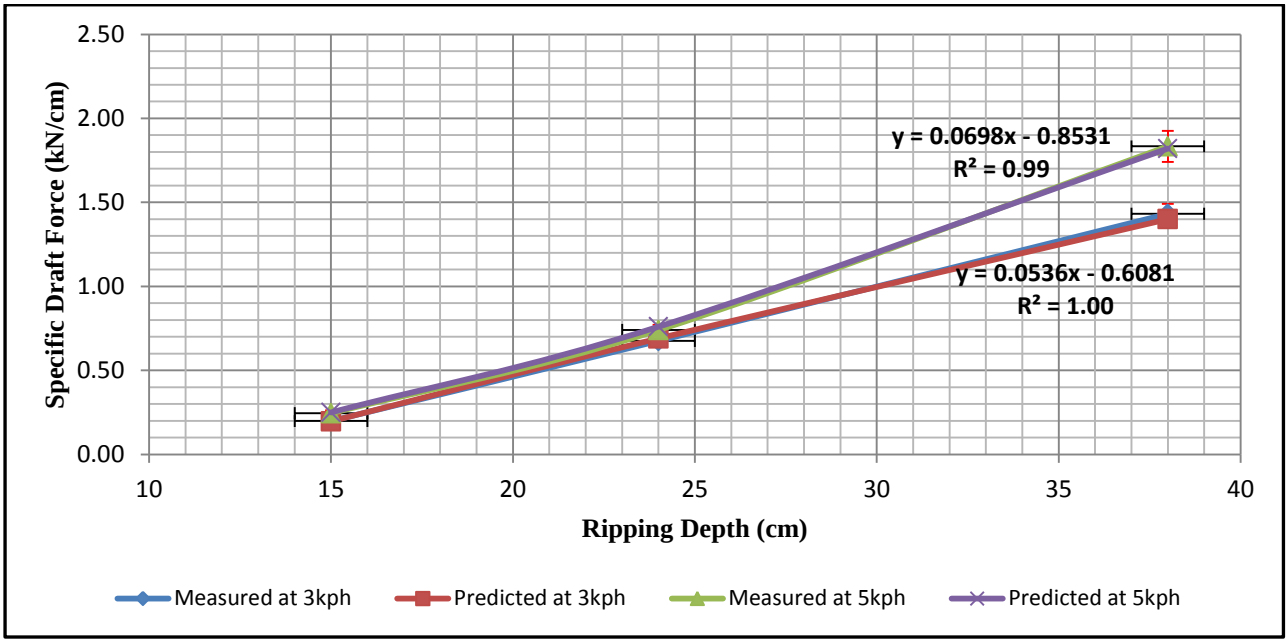


**Figure 5.7: Specific Draft Force against Ripping Depth at a Rake Angle of 45$^{o}$**

At the rake angle of 45 degrees, the measured and predicted specific draft increased linearly with the ripping depth. Increasing the ripping depth from 15cm to about 40cm resulted to an

increase in the specific draft by 1.23 kN/cm at the speed of 3 kph and by 1.59 kN/cm at the speed of 5kph.

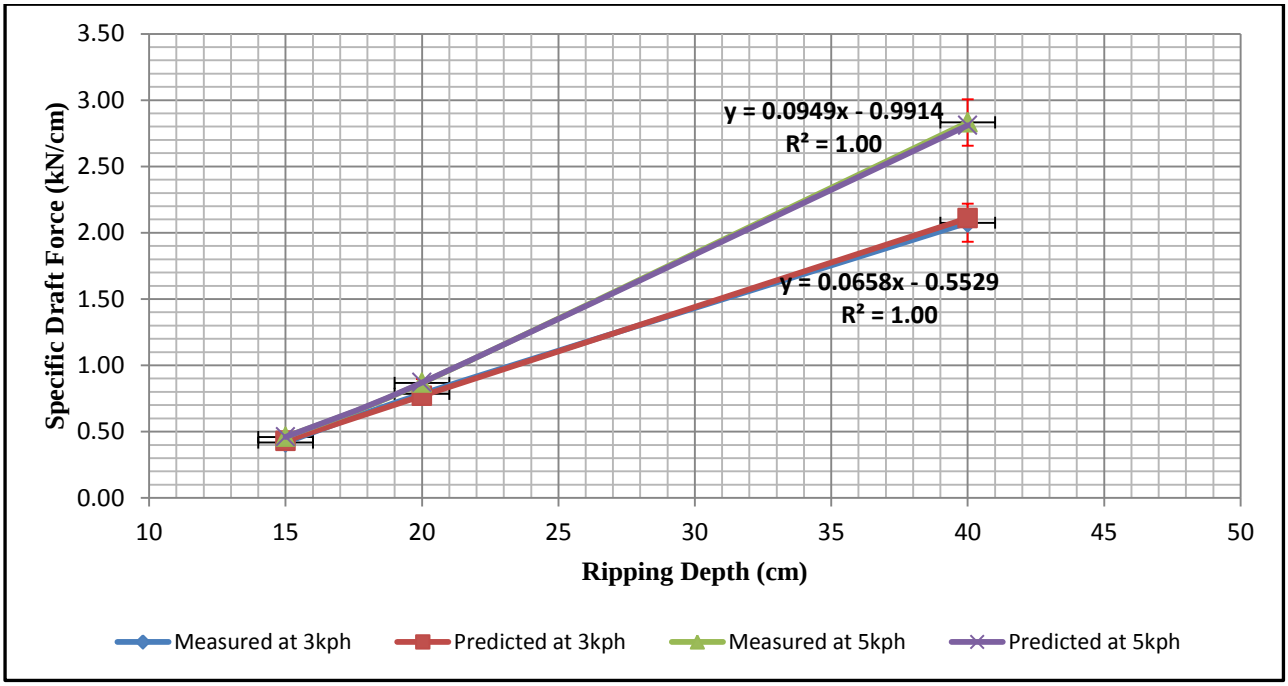


**Figure 5.8: Specific Draft Force against Ripping Depth at a Rake Angle of 60$^{o}$**

At the rake angle of 60 degrees, the measured and predicted specific draft increased linearly with the ripping depth. Increasing the ripping depth from 15cm to about 40cm resulted to an increase in the specific draft by 1.66 kN/cm at the speed of 3 kph and by 2.37 kN/cm at the speed of 5kph.

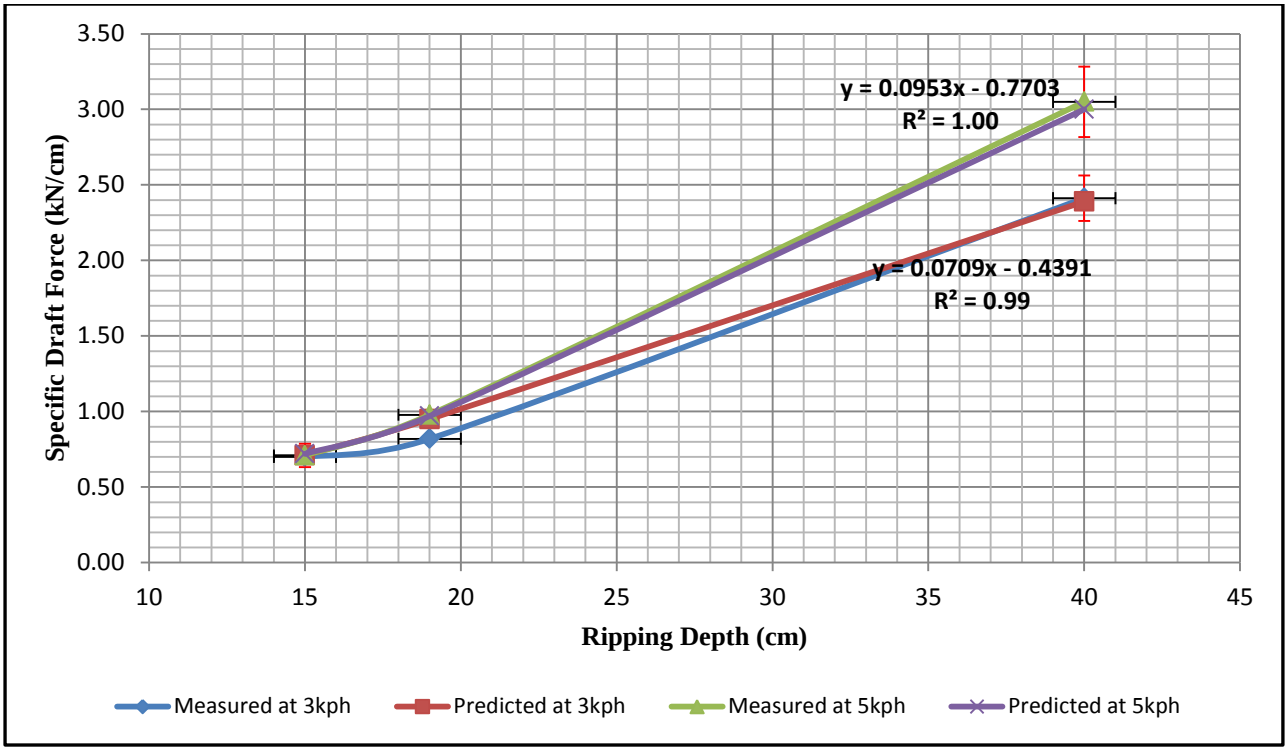


**Figure 5.9: Specific Draft Force against Ripping Depth at a Rake Angle of 75$^{o}$**

At the rake angle of 75 degrees, the measured and predicted specific draft increased linearly with the ripping depth. Increasing the ripping depth from 15cm to about 40cm resulted to an increase in the specific draft by 1.7 kN/cm at the speed of 3 kph and by 2.4 kN/cm at the speed of 5kph.

The draft has been shown to increase with an increase with the ripping depth; in his research to develop models for chisel plows using Artificial Neural Networks working with different soil conditions, Aboukarima (2007) found the draft to increase in a linear manner with the working depth. This was in agreement with the findings of Grisso & Perumpral (1985b) who reported a linear increase in the draft obtained using the Hettiaratchi & Reece (1967) model; they however obtained an exponential increase with the models developed by Godwin & Spoor (1977) and McKyes & Ali (1977).

### 5.6.3 Effect of Operating Speed

The effect of the operating speed on the draft has been investigated by various researchers (Onwualu & Watts, 1998; Sahu & Raheman, 2006; Aboukarima, 2007; Ghaly & Al-Suhaibani, 2010; Moeenifar *et al*., 2013). The general observation has been that increasing the operating speed results to an increase in the draft. Sahu & Raheman (2006) however report that the effect of changing the operating speed on the draft is less pronounced than the effect of changing the working depth on the draft.

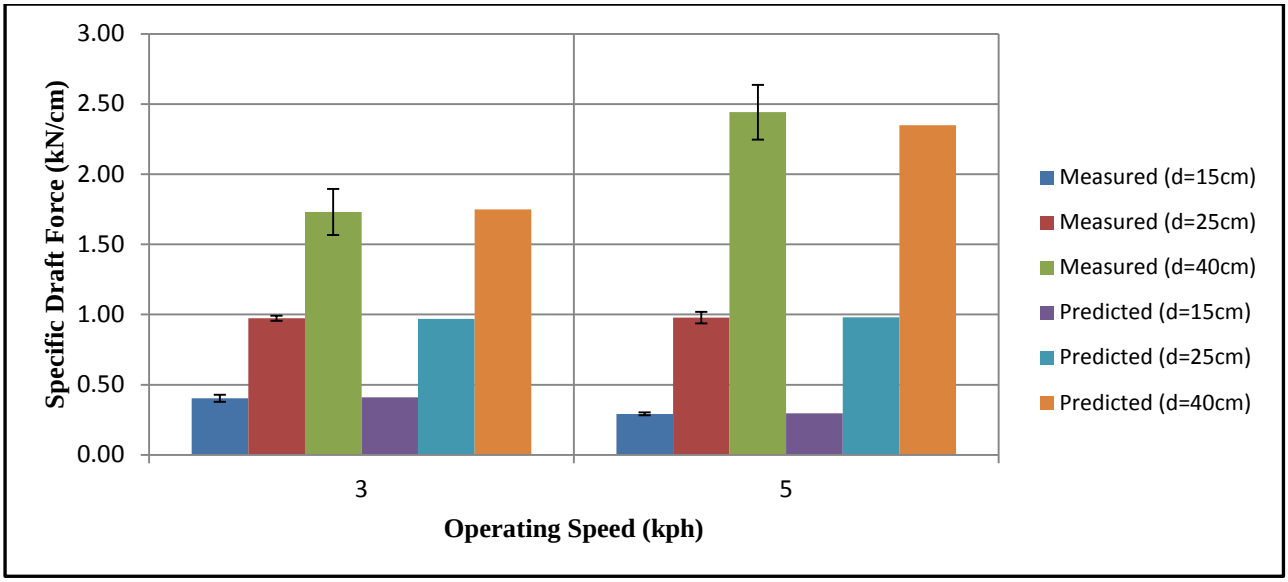


**Figure 5.10: Specific Draft Force against Operating Speed at a Rake Angle of 30$^{o}$**

Investigations at the rake angle of 30 degrees revealed that the effect of the change in operating speed on the draft was more prominent at the ripping depth of 40 cm than at the other depths. This could be due the presence of a loose soil layer at lower ripping depths as discussed in section 5.6.1.

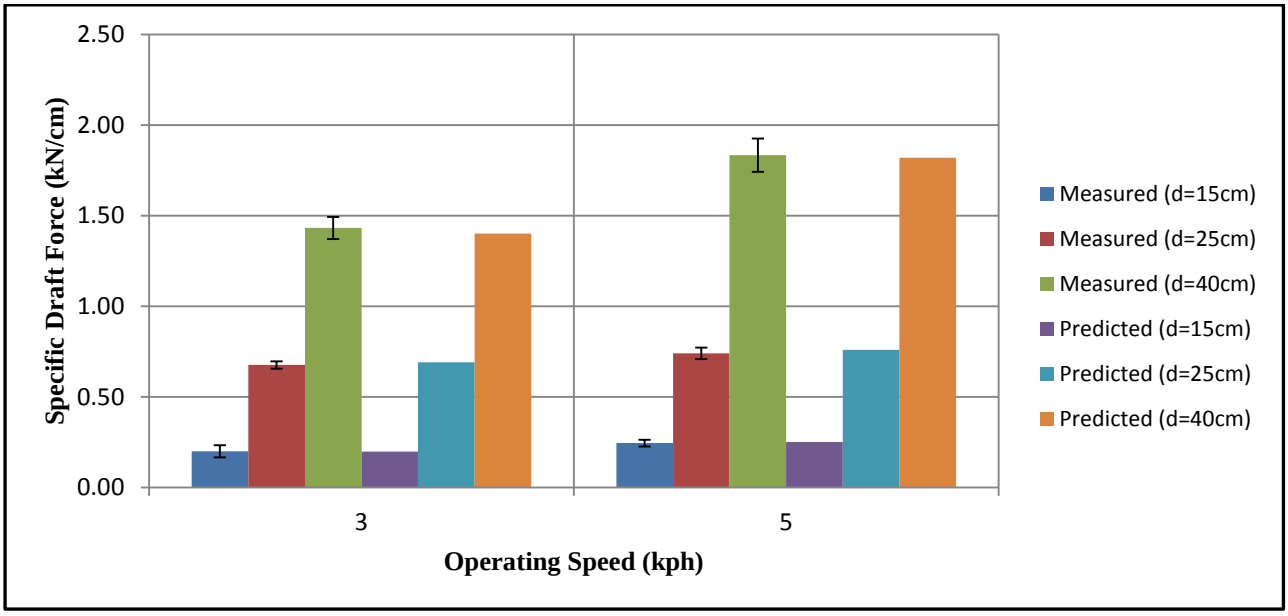


**Figure 5.11: Specific Draft Force against Operating Speed at a Rake Angle of 45$^{o}$**

At the rake angle of 45 degrees, the effect of the change in operating speed on the draft was again more prominent at the ripping depth of 40 cm than at the other depths. At ripping depths less than 40cm, the change in operating speed resulted to a marginal change in the draft.

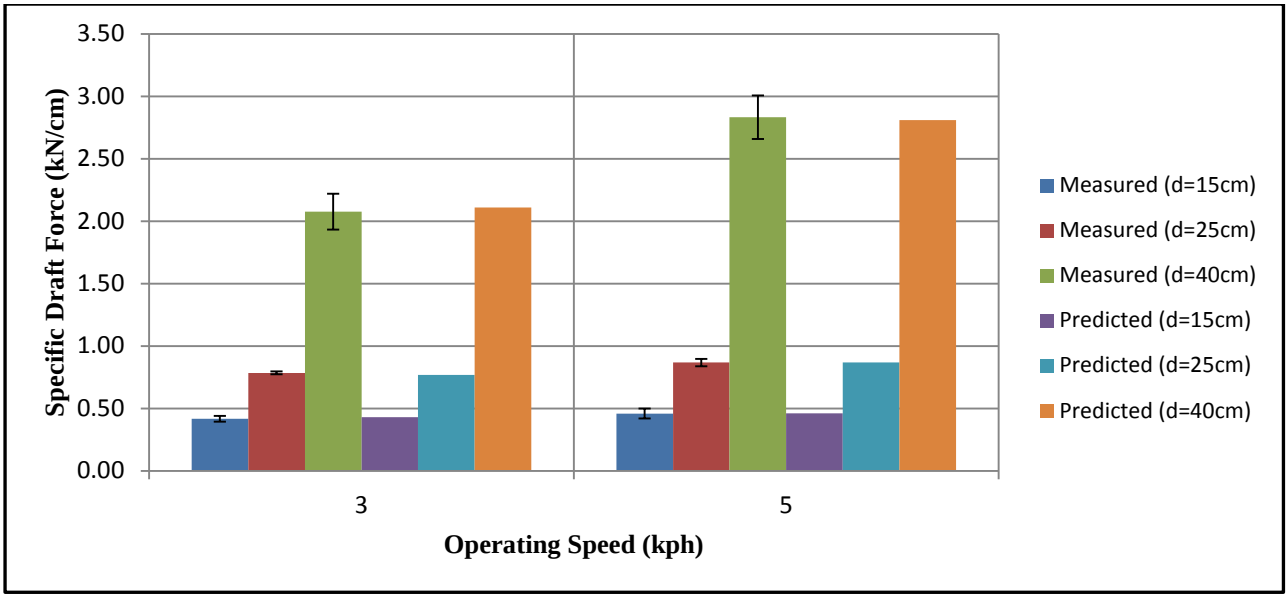


**Figure 5.12: Specific Draft Force against Operating Speed at a Rake Angle of 60$^{o}$**

At the rake angle of 60 degrees, the effect of the change in operating speed on the draft was again more prominent at the ripping depth of 40 cm than at the other depths. At ripping depths less than 40cm, the change in operating speed resulted to a marginal change in the draft.

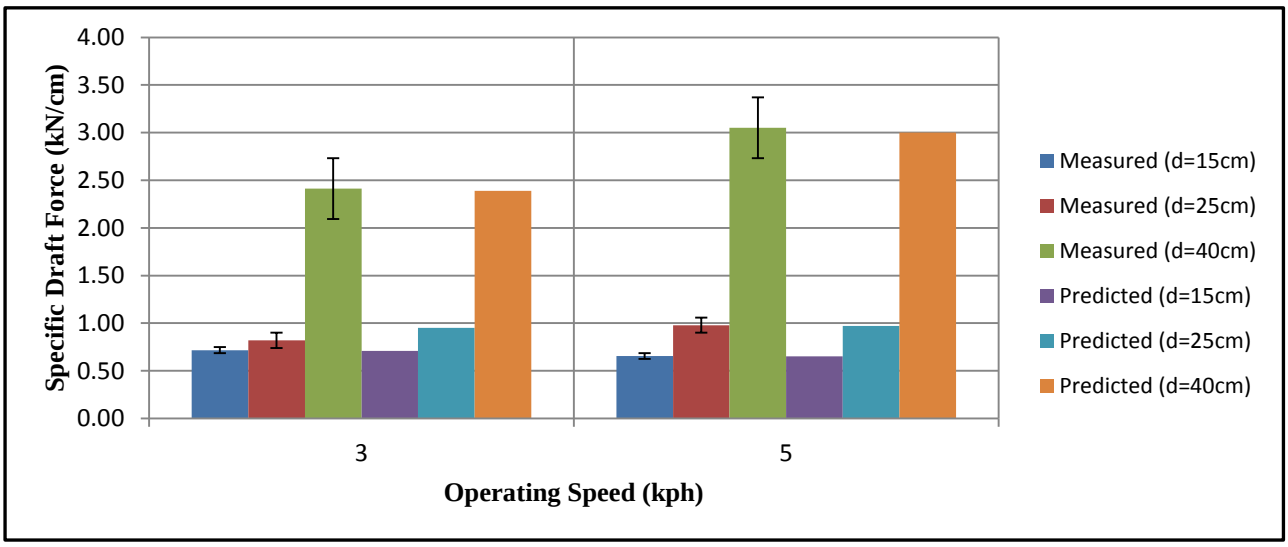


**Figure 5.13: Specific Draft Force against Operating Speed at a Rake Angle of 75$^{o}$**

At the rake angle of 75 degrees, the effect of the change in operating speed on the draft was again more prominent at the ripping depth of 40 cm than at the other depths. At ripping depths less than 40cm, the change in operating speed resulted to a marginal change in the draft.

# CHAPTER SIX: CONCLUSIONS AND RECOMMENDATIONS

## 6.1. Conclusions

The purpose of this study was to apply a numerical simulation model to predict the resistance to ripping in a sandy clay soil. The study aimed at investigating the applicability of the discrete element method in modelling soil-tool interaction in tillage studies particularly ripping processes. The information gained along the simulation model can be used to establish the draft forces arising out of a ripping operation; this information and model have potential applications in tillage research, tool design in the industry and tillage management by farm managers.

The measured and predicted draft datasets were investigated for normality using the One Sample Kolmogorov-Smirnov Test in SPSS; it was found out that both the datasets were normally distributed. Regression analysis for the two datasets was also conducted in SPSS to investigate their degree of fit; the datasets were found to correlate well with the coefficient of determination ($R^2$) of 0.986; this finding corroborated with the paired samples t-test in SPSS which indicated that the predicted draft dataset was significantly similar to the measured draft dataset at the 95% level of confidence; this implied that the developed simulation model was of high fidelity and that the calibration parameters obtained were a good representation of the actual field conditions; it was thus concluded that the simulation model accurately modelled the ripping process.

Statistical analysis established that differences in the experimental blocks influenced the measured draft force, however, the results of Block 1 were similar to those of Block 2 and the results of Block 3 were similar to those of Block 4; this could be because Block 1 and 2 where on the upper side of the experimental plot while Block 3 and 4 where on the lower side of the experimental plot. The effect of the differences in the experimental blocks was insignificant for the predicted draft force; this is because only the average soil parameters for all the blocks were used in the simulation to simplify the process.

Rake Angles were found to have a significant effect on both the measured and predicted draft force; it was found out that the draft force reduced with the rake angle of $30^o$ to attain a minimum value at a rake angle of $45^o$ then increased exponentially through the rake angle of

$60^o$ to attain a maximum value at the rake angle of $75^o$. The rake angle of $45^o$ thus presented the optimum value of rake angle that should be utilised for the minimum draft requirements.

Analysis of Variance found both the tillage depth and operational speed to influence the draft force at the 95% level of confidence; it was found out that the draft force was directly proportional to the tillage depth and operational speed as such, the draft force increased with increase in the two parameters. The critical depth of tillage was found to be at 34cm, as such, the draft force was found to be more sensitive to the tillage depth past the 34cm level since it was found to increase exponentially past that level. Only two speed levels (3km/hr and 5km/hr) were used in this study; the draft was not sensitive to the changes in speed level, further studies are recommended at finer speed level within the above range to make good observations on their effect on the draft force; however, most tillage operations are conducted within the range of 3km/hr (0.8 m/s) and 5km/hr (1.4 m/s) and as such, this study's observations at such a range are usable.

### 6.2. Recommendations

The following recommendations based on the findings of this research are made;

1. The angle of repose test was used to calibrate the numerical model; further studies should be done to establish the applicability of other tests, such as the triaxial test, in calibrating numerical models developed using EDEM Academic™;
2. The soil-tool interaction during soil cutting with a narrow ripper was investigated; this was done is a humic Nitisol (sandy clay soil); further studies should be directed at modeling the forces that arise during soil loosening with other tools such as the moldboard plough which is a commonly used tool in Kenyan farms. This study should be replicated in farms located in other soil types, particularly the black cotton soil;
3. Soil ripping in sandy clay soils should be conducted at the rake angle of $45^o$ to reduce the soil resistance.
4. Further studies should be conducted with rake angles outside the range of $30^o$ to $75^o$ since the rake angle of $45^o$ established to be the angle for the minimum draft force and $75^o$ established to be the angle for the maximum draft force were only the respective minimum and maximum within that particular range; there could be other rake angles outside the range that give different values of the minimum and maximum draft force.

## REFERENCES


Aboukarima, W. (2007). Draft models of chisel plow based on simulation using artificial neural networks. *Misr J. Ag. Eng.*, *24*(January 2007), 42–61.

Ardic, O. (2006). *Analysis of Bearing Capacity using Discrete Element Method*. Middle East Technical University.

Asaf, Z., Rubinstein, D., & Shmulevich, I. (2007). Determination of discrete element model parameters required for soil tillage. *Soil and Tillage Research*, *92*(1-2), 227–242. doi:10.1016/j.still.2006.03.006

Benites, J., Pisante, M., & Stagnari, F. (2005). Integrated Soil and Water Management for Orchard Development. In *International Seminar on the Role and Importance of Integrated Soil and Water Management for Orchard Development* (p. 154). Food & Agriculture Org. Retrieved from http://books.google.com/books?id=aaedifm87S4C&pgis=1

Blanco-Canqui, H. (2008). *Principles of Soil Conservation and Management (Google eBook)*. Springer. Retrieved from http://books.google.com/books?id=Wj3690PbDY0C&pgis=1

Cundall, P. ., & Strack, O. D. . (1979). A discrete numerical model for granular assemblies. *Geotechnique*, *1*(29).

Dedousis, A., & Bartzanas, T. (2010). *Soil Engineering (Google eBook)*. Springer. Retrieved from http://books.google.com/books?id=AyLNvwX9hzcC&pgis=1

DEM Solutions Limited. (2014). EDEM 2.6 User Guide. Edinburgh.

Gachene, C., Jarvis, N., Linner, H., & Mbuvi, J. (2000). *Soil erosion effects on productivity of a humic nitisol*. Retrieved from http://agris.fao.org/agris-search/search/display.do?f=2008/KE/KE0702.xml;KE2007200229

Ghaly, A., & Al-Suhaibani, S. (2010). Effect of Plowing Depth of Tillage and Forward Speed on the Performance of a Medium Size Chisel Plow Operating in a Sandy Soil. *American Journal of Agricultural and Biological Sciences*, *5*(3), 247–255.

Gill, W. R., & Vandeberg, G. . (1968). Soil Dynamics in Tillage and Traction in Agriculture, *Agriculture*(316).

Gitau, A. ., & Gumbe, L. . (2004). Alleviating soil hardpan formation for conservation farming –case of semi-arid Kenya. *Euro-Asia Journal of Applied Sciences*, *2*(3).

Gitau, A. ., Gumbe, L. ., & Biamah, E. . (2006). Influence of soil water on stress-strain behaviour of a compacting irrigatable soil in semi-arid Kenya. *Elsevier*, *89*.

Godwin, R. J., & O'Dogherty, M. J. (2007). Integrated soil tillage force prediction models. *Journal of Terramechanics*, *44*(1), 3–14. doi:10.1016/j.jterra.2006.01.001

Godwin, R. J., & Spoor, G. (1977). Soil failure with narrow tines. *Journal of Agricultural Engineering*, *22*(4), 213–228.

Grisso, R. D., & Perumpral, J. V. (1985a). *Review of Models for Predicting Performance of Narrow Tillage Tool* (Vol. 7).

Grisso, R. D., & Perumpral, J. V. (1985b). Review of Models for Predicting Performance of Narrow Tillage Tool, *7*.

Hettiaratchi, D. R. ., & Reece, A. . (1967). Symmetrical three-dimensional soil failure. *Journal of Terramechanics*, *4*(3), 45–67.

Huang, H. (2010). *Discrete Element Modeling of Railroad Ballast using Image-based Aggregate Morphology Characterization*. University of Illinois at Urbana-Champaign.

Huang, H. A. I. (2010). *Discrete Element Modeling of Railroad Ballast using Imaging Based Aggregate Morphology Characterization*.

Karmakar, S. (2005). *Numerical modeling of soil flow and pressure distribution on a simple tillage tool using Computational Fluid Dynamics*. University of Sasketchewan.

Karmakar, S., Ashrafizadeh, S. R., & Kushwaha, R. L. (2009). Experimental validation of computational fluid dynamics modeling for narrow tillage tool draft. *Journal of Terramechanics*, *46*(6), 277–283. doi:10.1016/j.jterra.2009.06.001

Karuku, G., Gachene, C., Karanja, N., Cornelis, W., Verplancke, H., & Kironchi, G. (2012). Soil hydraulic properties of a Nitisol in Kabete Kenya. *Tropical and Subtropical Agroecosystems*, *15*, 595–609.

Kasisira, L. L. (2004). *Force Modelling and Energy Optimization for Subsoilers in Tandem*. University of Pretoria.

Lichtfouse, E. (2010). *Biodiversity, Biofuels, Agroforestry and Conservation Agriculture (Google eBook)*. Springer. Retrieved from http://books.google.com/books?id=XiGNuikzGU0C&pgis=1

Linde, J. (2007). *Discrete Element Modeling of a Vibratory Subsoiler*. University of Stellenbosch.

Losada, M., Rodriguez, R., & MacAdam, J. (2005). *Silvopastoralism and Sustainable Land Management (Google eBook)*. CABI. Retrieved from http://books.google.com/books?id=RGkdPxcL_2sC&pgis=1

Lull, H. W. (1959). *Soil Compaction on Forest and Range Lands (Google eBook)*. Forest Service, U.S. Department of Agriculture. Retrieved from http://books.google.com/books?id=OSsuAAAAYAAJ&pgis=1

Majidi, B. (2012). *Discrete Element Method Applied to the Vibration Process of Coke Particles*. University of Quebec.

Marenya, M. O. (2009). *Performance characteristics of a deep tilling rotavator Performance characteristics of a deep tilling rotavator*. University of Pretoria.

Maswaure, J. (1995). *Tillage Forces and Soil Loosening as Influenced by Tool Geometry*. McGill University.

McKyes, E., & Ali, O. . (1977). The cutting of soil by narrow blades. *Journal of Terramechanics*, *14*(2), 43–58.

Milovac, J. (2009). *Rock Physics Modeling of an Unconsolidated Sand Reservoir*. University of Houston.

Moeenifar, A., Seyedi, S. R., & Kalantari, D. (2013). Determination of traction force acting on a wide blade using dimensional analysis method. *IJACS*, 1403–1409.

Nawaz, M. F., Bourrié, G., & Trolard, F. (2012). Soil compaction impact and modelling. A review. *Agronomy for Sustainable Development*, *33*(2), 291–309. doi:10.1007/s13593-011-0071-8

O'Callaghan, J., & Farrelly, K. (1964). Cleavage of soil by tined implements. *Journal of Agricultural Engineering Research*, *9*(3), 259–270.

Obermayr, M., Dressler, K., Vrettos, C., & Eberhard, P. (2011). Prediction of draft forces in cohesionless soil with the Discrete Element Method. *Journal of Terramechanics*, *48*(5), 347–358. doi:10.1016/j.jterra.2011.08.003

Obermayr, M., Vrettos, C., Kleinert, J., & Eberhard, P. (2013). A Discrete Element Method for assessing reaction forces in excavationtools. *Berichte Des Fraunhofer*.

Okayasu, T., Morishita, K., Terao, H., Mitsuoka, M., Inoue, E., & Fukami, K. (2010). Modeling and Prediction of Soil Cutting Behavior by a Plow Frictional slider, 1–6.

Onwualu, A. P., & Watts, K. C. (1998). Draught and vertical forces obtained from dynamic soil cutting by plane tillage tools. *Soil & Tillage Research*, *48*, 251.

Osman, J. . (1964). The mechanics of soil cutting blades. *Journal of Agricultural Engineering Research*, *9*(4), 313–328.

Payne, J. M. (2008). *Identification of Subsoil Compaction Using Electrical Conductivity and Spectral Data Across Varying Soil Moisture Regimes in Utah*. ProQuest. Retrieved from http://books.google.com/books?id=V8Q27MC9vKkC&pgis=1

Payne, P. (1956). The relationship between the mechanical properties of soil and the performance of simple cultivation implements. *Journal of Agricultural Engineering Research*, *1*(1), 23–50.

Penn State Extension. (n.d.). *Soil Compaction Agronomy Guide*. Retrieved from http://extension.psu.edu/agronomy-guide/cm/sec1/sec11f

Perumpral, J. ., Grisso, R. ., & Desai, C. . (1983). A soil-tool model based on limit equilibrium analysis. *TRANSACTIONS of the ASAE*, *26*(4), 991–995.

Raj, P. P. (2008). *Soil Mechanics & Foundation Engineering*. Pearson Education India. Retrieved from http://books.google.com/books?id=j9MhMcsGcOUC&pgis=1

Rose, C. W. (2004). *An Introduction to the Environmental Physics of Soil, Water and Watersheds*. Cambridge University Press. Retrieved from http://books.google.com/books?id=TxCQ-DaSIwUC&pgis=1

Sahu, R. K., & Raheman, H. Ã. (2006). Draught Prediction of Agricultural Implements using Reference Tillage Tools in Sandy Clay Loam Soil. *Biosystems Engineering*, *94*, 275–284. doi:10.1016/j.biosystemseng.2006.01.015

Schmeiser Farm Equipment. (2014). *Vineyard Rippers*. Retrieved June 3, 2015, from www.tgschmeiser.com/products/rippers/vr.html

Shmulevich, I. (2010). State of the art modeling of soil–tillage interaction using discrete element method. *Soil and Tillage Research*, *111*(1), 41–53. doi:10.1016/j.still.2010.08.003

Shmulevich, I., Asaf, Z., & Rubinstein, D. (2007). Interaction between soil and a wide cutting blade using the discrete element method. *Soil and Tillage Research*, *97*(1), 37–50. doi:10.1016/j.still.2007.08.009

Sitharam, T. (2000). Numerical simulation of particulate materials using discrete element modeling. *Current Science*, *78*(7).

Smith, M., Collis, L., & Fookes, P. . (2001). *Aggregates: Sand, Gravel and Crushed Rock Aggregates for Construction Purposes*. Geological Society of London.

Swick, W. ., & Perumpral, J. . (1988). A model for predicting soil-tool interaction. *Journal of Terramechanics*, *25*(1), 43–56.

Tong, J., & Moayad, B. Z. (2006). Effects of rake angle of chisel plough on soil cutting factors and power requirements: A computer simulation. *Soil and Tillage Research*, *88*(1-2), 55–64. doi:10.1016/j.still.2005.04.007

Urbán, M., Kotrocz, K., & Kerényi, G. (2002). Investigation of the soil - tool interaction by SPH ( Smooth Particle Hydrodynamics ) based simulation.

Wiebe, K. (2003). *Land Quality, Agricultural Productivity, and Food Security: Biophysical Processes and Economic Choices at Local, Regional, and Global Levels (Google eBook)*. Edward Elgar Publishing. Retrieved from http://books.google.com/books?id=lZV4lU1fFAgC&pgis=1

Zadeh, S. (2006). *Modelling of Energy Requirements by a Narrow Tillage Tool*. University of Sasketchewan.

Zeng, D., & Yao, Y. (1992). A dynamic model for soil cutting by blade and tine. *Journal of Terramechanics*, *29*(3), 317–327.

# APPENDICES

## APPENDIX A: GLOSSARY

| Term | Definition |
|---|---|
| **Ripper** | A chisel-shaped agricultural implement that can be animal or tractor powered. It breaks up and opens a narrow slot or furrow in the soil to loosen and aerate the soil while leaving crop residue at the top of the soil without overturning the soil |
| **Critical depth** | A depth that depends on the slenderness of a tillage tool below which soil compaction other than loosening occurs |
| **Dynamometer** | A force measuring device that operates in both the horizontal and vertical axes without taking lateral forces |
| **Gravimetric Analysis** | Analysis based on mass/ weight measurements |
| **Tillage** | This is the preparation of soil for agricultural purposes by mechanical agitation of various types, such as digging, stirring, and overturning. |
| **Tine** | A 'prong' on an agricultural tool or similar implement characterized by an end that is more or less sharp or pointed |
| **Prototype** | An early sample, model, or release of a product built to test a concept or process or to act as a thing to be replicated or learned from |
| **Draft** | This is the pull required to operate an agricultural tool or generated by a prime mover to pull an agricultural tool |
| **Iteration** | Is the act of repeating a process with the aim of approaching a desired goal, target or result |
| **Angle of Repose** | The steepest angle at which a sloping surface formed of a particular loose material is stable. |
| **Tab** | Is a feature in a software program window and in an Internet browser, which allows for the user to access different parts of a menu or program window |
| **Young's** | Is the ratio of the stress (force per unit area) along an axis to the strain |

| | |
|---|---|
| **modulus** | (ratio of deformation over initial length) along that axis in the range of stress in which Hooke's law holds |
| **Shear Modulus** | Is the ratio of shear stress to the shear strain |
| **Poisson's Ratio** | Is the ratio of transverse contraction strain to longitudinal extension strain in the direction of the stretching force |
| **Surface Energy** | Is the work per unit area done by the force that creates the new surface |
| **Work Function** | Is the minimum thermodynamic work needed to remove an electron from a solid to a point in the vacuum immediately outside the solid surface |

## APPENDIX B: SPECIFIC DRAFT DATA

| Block | Speed (kph) | Rake Angle (degrees) | Depth (cm) | Measured Specific Draft (kN/cm) | Predicted Specific Draft (kN/cm) |
|---|---|---|---|---|---|
| Block 1 | 3 | 30 | 15 | 0.39 | 0.41 |
| Block 1 | 3 | 30 | 25 | 0.95 | 0.97 |
| Block 1 | 3 | 30 | 40 | 1.56 | 1.75 |
| Block 1 | 3 | 45 | 15 | 0.18 | 0.20 |
| Block 1 | 3 | 45 | 25 | 0.65 | 0.69 |
| Block 1 | 3 | 45 | 40 | 1.38 | 1.40 |
| Block 1 | 3 | 60 | 15 | 0.40 | 0.43 |
| Block 1 | 3 | 60 | 25 | 0.78 | 0.77 |
| Block 1 | 3 | 60 | 40 | 1.97 | 2.11 |
| Block 1 | 3 | 75 | 15 | 0.74 | 0.71 |
| Block 1 | 3 | 75 | 25 | 0.80 | 0.82 |
| Block 1 | 3 | 75 | 40 | 2.28 | 2.39 |
| Block 1 | 5 | 30 | 15 | 0.28 | 0.30 |
| Block 1 | 5 | 30 | 25 | 0.93 | 0.98 |
| Block 1 | 5 | 30 | 40 | 2.39 | 2.35 |
| Block 1 | 5 | 45 | 15 | 0.22 | 0.25 |
| Block 1 | 5 | 45 | 25 | 0.70 | 0.76 |
| Block 1 | 5 | 45 | 40 | 1.79 | 1.82 |
| Block 1 | 5 | 60 | 15 | 0.43 | 0.46 |
| Block 1 | 5 | 60 | 25 | 0.83 | 0.87 |
| Block 1 | 5 | 60 | 40 | 2.71 | 2.81 |
| Block 1 | 5 | 75 | 15 | 0.62 | 0.65 |
| Block 1 | 5 | 75 | 25 | 0.94 | 0.97 |
| Block 1 | 5 | 75 | 40 | 2.94 | 3.00 |
| Block 2 | 3 | 30 | 15 | 0.37 | 0.41 |
| Block 2 | 3 | 30 | 25 | 0.99 | 0.97 |
| Block 2 | 3 | 30 | 40 | 1.59 | 1.75 |
| Block 2 | 3 | 45 | 15 | 0.16 | 0.20 |
| Block 2 | 3 | 45 | 25 | 0.66 | 0.69 |
| Block 2 | 3 | 45 | 40 | 1.39 | 1.40 |
| Block 2 | 3 | 60 | 15 | 0.39 | 0.43 |
| Block 2 | 3 | 60 | 25 | 0.80 | 0.77 |
| Block 2 | 3 | 60 | 40 | 1.97 | 2.11 |

| | | | | | |
|---|---|---|---|---|---|
| Block 2 | 3 | 75 | 15 | 0.73 | 0.71 |
| Block 2 | 3 | 75 | 25 | 0.83 | 0.82 |
| Block 2 | 3 | 75 | 40 | 2.29 | 2.39 |
| Block 2 | 5 | 30 | 15 | 0.30 | 0.30 |
| Block 2 | 5 | 30 | 25 | 0.97 | 0.98 |
| Block 2 | 5 | 30 | 40 | 2.31 | 2.35 |
| Block 2 | 5 | 45 | 15 | 0.25 | 0.25 |
| Block 2 | 5 | 45 | 25 | 0.75 | 0.76 |
| Block 2 | 5 | 45 | 40 | 1.82 | 1.82 |
| Block 2 | 5 | 60 | 15 | 0.45 | 0.46 |
| Block 2 | 5 | 60 | 25 | 0.85 | 0.87 |
| Block 2 | 5 | 60 | 40 | 2.86 | 2.81 |
| Block 2 | 5 | 75 | 15 | 0.63 | 0.65 |
| Block 2 | 5 | 75 | 25 | 0.99 | 0.97 |
| Block 2 | 5 | 75 | 40 | 2.99 | 3.00 |
| Block 3 | 3 | 30 | 15 | 0.41 | 0.41 |
| Block 3 | 3 | 30 | 25 | 0.96 | 0.97 |
| Block 3 | 3 | 30 | 40 | 1.96 | 1.75 |
| Block 3 | 3 | 45 | 15 | 0.25 | 0.20 |
| Block 3 | 3 | 45 | 25 | 0.69 | 0.69 |
| Block 3 | 3 | 45 | 40 | 1.53 | 1.40 |
| Block 3 | 3 | 60 | 15 | 0.43 | 0.43 |
| Block 3 | 3 | 60 | 25 | 0.79 | 0.77 |
| Block 3 | 3 | 60 | 40 | 2.32 | 2.11 |
| Block 3 | 3 | 75 | 15 | 0.68 | 0.71 |
| Block 3 | 3 | 75 | 25 | 0.82 | 0.82 |
| Block 3 | 3 | 75 | 40 | 2.65 | 2.39 |
| Block 3 | 5 | 30 | 15 | 0.30 | 0.30 |
| Block 3 | 5 | 30 | 25 | 1.04 | 0.98 |
| Block 3 | 5 | 30 | 40 | 2.30 | 2.35 |
| Block 3 | 5 | 45 | 15 | 0.27 | 0.25 |
| Block 3 | 5 | 45 | 25 | 0.73 | 0.76 |
| Block 3 | 5 | 45 | 40 | 1.74 | 1.82 |
| Block 3 | 5 | 60 | 15 | 0.53 | 0.46 |
| Block 3 | 5 | 60 | 25 | 0.89 | 0.87 |
| Block 3 | 5 | 60 | 40 | 2.65 | 2.81 |
| Block 3 | 5 | 75 | 15 | 0.79 | 0.65 |

| | | | | | |
|---|---|---|---|---|---|
| Block 3 | 5 | 75 | 25 | 1.01 | 0.97 |
| Block 3 | 5 | 75 | 40 | 2.83 | 3.00 |
| Block 4 | 3 | 30 | 15 | 0.44 | 0.41 |
| Block 4 | 3 | 30 | 25 | 0.99 | 0.97 |
| Block 4 | 3 | 30 | 40 | 1.81 | 1.75 |
| Block 4 | 3 | 45 | 15 | 0.21 | 0.20 |
| Block 4 | 3 | 45 | 25 | 0.70 | 0.69 |
| Block 4 | 3 | 45 | 40 | 1.44 | 1.40 |
| Block 4 | 3 | 60 | 15 | 0.45 | 0.43 |
| Block 4 | 3 | 60 | 25 | 0.77 | 0.77 |
| Block 4 | 3 | 60 | 40 | 2.04 | 2.11 |
| Block 4 | 3 | 75 | 15 | 0.72 | 0.71 |
| Block 4 | 3 | 75 | 25 | 0.83 | 0.82 |
| Block 4 | 3 | 75 | 40 | 2.43 | 2.39 |
| Block 4 | 5 | 30 | 15 | 0.29 | 0.30 |
| Block 4 | 5 | 30 | 25 | 0.97 | 0.98 |
| Block 4 | 5 | 30 | 40 | 2.77 | 2.35 |
| Block 4 | 5 | 45 | 15 | 0.23 | 0.25 |
| Block 4 | 5 | 45 | 25 | 0.79 | 0.76 |
| Block 4 | 5 | 45 | 40 | 1.99 | 1.82 |
| Block 4 | 5 | 60 | 15 | 0.43 | 0.46 |
| Block 4 | 5 | 60 | 25 | 0.90 | 0.87 |
| Block 4 | 5 | 60 | 40 | 3.11 | 2.81 |
| Block 4 | 5 | 75 | 15 | 0.59 | 0.65 |
| Block 4 | 5 | 75 | 25 | 0.97 | 0.97 |
| Block 4 | 5 | 75 | 40 | 3.44 | 3.00 |

## APPENDIX C: CALIBRATION PARAMETERS

| Simulation No. | Simulation File name | JKR Energy ($J/m^2$) | Coefficient of Restitution | Coefficient of Static Friction | Coefficient of Rolling Friction | Angle of Repose |
|---|---|---|---|---|---|---|
| 1. | 5-0.1-0.2-0.06 | 5 | 0.1 | 0.2 | 0.06 | $26.75^o$ |
| 2. | 5-0.1-0.2-0.12 | 5 | 0.1 | 0.2 | 0.12 | $22.92^o$ |
| 3. | 5-0.1-0.4-0.06 | 5 | 0.1 | 0.4 | 0.06 | $15.57^o$ |
| 4. | 5-0.1-0.4-0.12 | 5 | 0.1 | 0.4 | 0.12 | $11.84^o$ |
| 5. | 5-0.1-0.6-0.06 | 5 | 0.1 | 0.6 | 0.06 | $7.78^o$ |
| 6. | 5-0.1-0.6-0.12 | 5 | 0.1 | 0.6 | 0.12 | $25.18^o$ |
| 7. | 5-0.2-0.2-0.06 | 5 | 0.2 | 0.2 | 0.06 | $15.22^o$ |
| 8. | 5-0.2-0.2-0.12 | 5 | 0.2 | 0.2 | 0.12 | $15.72^o$ |
| 9. | 5-0.2-0.4-0.06 | 5 | 0.2 | 0.4 | 0.06 | $33.6^o$ |
| 10. | 5-0.2-0.4-0.12 | 5 | 0.2 | 0.4 | 0.12 | $31.68^o$ |
| 11. | 5-0.2-0.6-0.06 | 5 | 0.2 | 0.6 | 0.06 | $32.72^o$ |
| 12. | 5-0.2-0.6-0.12 | 5 | 0.2 | 0.6 | 0.12 | $28.03^o$ |
| 13. | 5-0.3-0.2-0.06 | 5 | 0.3 | 0.2 | 0.06 | Sticky |
| 14. | 5-0.3-0.2-0.12 | 5 | 0.3 | 0.2 | 0.12 | Sticky |
| 15. | 5-0.3-0.4-0.06 | 5 | 0.3 | 0.4 | 0.06 | Sticky |
| 16. | 5-0.3-0.4-0.12 | 5 | 0.3 | 0.4 | 0.12 | Sticky |
| 17. | 5-0.3-0.6-0.06 | 5 | 0.3 | 0.6 | 0.06 | Sticky |
| 18. | 5-0.3-0.6-0.12 | 5 | 0.3 | 0.6 | 0.12 | Sticky |
| 19. | 5-0.4-0.2-0.06 | 5 | 0.4 | 0.2 | 0.06 | Sticky |
| 20. | 5-0.4-0.2-0.12 | 5 | 0.4 | 0.2 | 0.12 | Sticky |
| 21. | 5-0.4-0.4-0.06 | 5 | 0.4 | 0.4 | 0.06 | Sticky |
| 22. | 5-0.4-0.4-0.12 | 5 | 0.4 | 0.4 | 0.12 | Sticky |
| 23. | 5-0.4-0.6-0.06 | 5 | 0.4 | 0.6 | 0.06 | Sticky |
| 24. | 5-0.4-0.6-0.12 | 5 | 0.4 | 0.6 | 0.12 | Sticky |
| 25. | 10-0.1-0.2-0.06 | 10 | 0.1 | 0.2 | 0.06 | $12.73^o$ |
| 26. | 10-0.1-0.2-0.12 | 10 | 0.1 | 0.2 | 0.12 | $8.96^o$ |
| 27. | 10-0.1-0.4-0.06 | 10 | 0.1 | 0.4 | 0.06 | $5.19^o$ |
| 28. | 10-0.1-0.4-0.12 | 10 | 0.1 | 0.4 | 0.12 | $4.86^o$ |
| 29. | 10-0.1-0.6-0.06 | 10 | 0.1 | 0.6 | 0.06 | $4.05^o$ |
| 30. | 10-0.1-0.6-0.12 | 10 | 0.1 | 0.6 | 0.12 | $4.18^o$ |
| 31. | 10-0.2-0.2-0.06 | 10 | 0.2 | 0.2 | 0.06 | $25.32^o$ |
| 32. | 10-0.2-0.2-0.12 | 10 | 0.2 | 0.2 | 0.12 | $19.94^o$ |

| | | | | | | |
|---|---|---|---|---|---|---|
| 33. | 10-0.2-0.4-0.06 | 10 | 0.2 | 0.4 | 0.06 | 28.96$^{o}$ |
| 34. | 10-0.2-0.4-0.12 | 10 | 0.2 | 0.4 | 0.12 | 20.28$^{o}$ |
| 35. | 10-0.2-0.6-0.06 | 10 | 0.2 | 0.6 | 0.06 | 17.04$^{o}$ |
| 36. | 10-0.2-0.6-0.12 | 10 | 0.2 | 0.6 | 0.12 | 24.78$^{o}$ |
| 37. | 10-0.3-0.2-0.06 | 10 | 0.3 | 0.2 | 0.06 | Sticky |
| 38. | 10-0.3-0.2-0.12 | 10 | 0.3 | 0.2 | 0.12 | Sticky |
| 39. | 10-0.3-0.4-0.06 | 10 | 0.3 | 0.4 | 0.06 | Sticky |
| 40. | 10-0.3-0.4-0.12 | 10 | 0.3 | 0.4 | 0.12 | Sticky |
| 41. | 10-0.3-0.6-0.06 | 10 | 0.3 | 0.6 | 0.06 | Sticky |
| 42. | 10-0.3-0.6-0.12 | 10 | 0.3 | 0.6 | 0.12 | Sticky |
| 43. | 10-0.4-0.2-0.06 | 10 | 0.4 | 0.2 | 0.06 | Sticky |
| 44. | 10-0.4-0.2-0.12 | 10 | 0.4 | 0.2 | 0.12 | Sticky |
| 45. | 10-0.4-0.4-0.06 | 10 | 0.4 | 0.4 | 0.06 | Sticky |
| 46. | 10-0.4-0.4-0.12 | 10 | 0.4 | 0.4 | 0.12 | Sticky |
| 47. | 10-0.4-0.6-0.06 | 10 | 0.4 | 0.6 | 0.06 | Sticky |
| 48. | 10-0.4-0.6-0.12 | 10 | 0.4 | 0.6 | 0.12 | Sticky |
| 49. | 15-0.1-0.2-0.06 | 15 | 0.1 | 0.2 | 0.06 | 16.99$^{o}$ |
| 50. | 15-0.1-0.2-0.12 | 15 | 0.1 | 0.2 | 0.12 | 13.69$^{o}$ |
| 51. | 15-0.1-0.4-0.06 | 15 | 0.1 | 0.4 | 0.06 | 9.15$^{o}$ |
| 52. | 15-0.1-0.4-0.12 | 15 | 0.1 | 0.4 | 0.12 | 16.24$^{o}$ |
| 53. | 15-0.1-0.6-0.06 | 15 | 0.1 | 0.6 | 0.06 | 4.33$^{o}$ |
| 54. | 15-0.1-0.6-0.12 | 15 | 0.1 | 0.6 | 0.12 | 5.43$^{o}$ |
| 55. | 15-0.2-0.2-0.06 | 15 | 0.2 | 0.2 | 0.06 | 19.39$^{o}$ |
| 56. | 15-0.2-0.2-0.12 | 15 | 0.2 | 0.2 | 0.12 | 36.15$^{o}$ |
| 57. | 15-0.2-0.4-0.06 | 15 | 0.2 | 0.4 | 0.06 | 24.22$^{o}$ |
| 58. | 15-0.2-0.4-0.12 | 15 | 0.2 | 0.4 | 0.12 | 28.67$^{o}$ |
| 59. | 15-0.2-0.6-0.06 | 15 | 0.2 | 0.6 | 0.06 | 18.93$^{o}$ |
| 60. | 15-0.2-0.6-0.12 | 15 | 0.2 | 0.6 | 0.12 | 19.78$^{o}$ |
| 61. | 15-0.3-0.2-0.06 | 15 | 0.3 | 0.2 | 0.06 | Sticky |
| 62. | 15-0.3-0.2-0.12 | 15 | 0.3 | 0.2 | 0.12 | Sticky |
| 63. | 15-0.3-0.4-0.06 | 15 | 0.3 | 0.4 | 0.06 | Sticky |
| 64. | 15-0.3-0.4-0.12 | 15 | 0.3 | 0.4 | 0.12 | Sticky |
| 65. | 15-0.3-0.6-0.06 | 15 | 0.3 | 0.6 | 0.06 | Sticky |
| 66. | 15-0.3-0.6-0.12 | 15 | 0.3 | 0.6 | 0.12 | Sticky |
| 67. | 15-0.4-0.2-0.06 | 15 | 0.4 | 0.2 | 0.06 | Sticky |
| 68. | 15-0.4-0.2-0.12 | 15 | 0.4 | 0.2 | 0.12 | Sticky |
| 69. | 15-0.4-0.4-0.06 | 15 | 0.4 | 0.4 | 0.06 | Sticky |

| | | | | | | |
|---|---|---|---|---|---|---|
| 70. | 15-0.4-0.4-0.12 | 15 | 0.4 | 0.4 | 0.12 | Sticky |
| 71. | 15-0.4-0.6-0.06 | 15 | 0.4 | 0.6 | 0.06 | Sticky |
| 72. | 15-0.4-0.6-0.12 | 15 | 0.4 | 0.6 | 0.12 | Sticky |
| 73. | 20-0.1-0.2-0.06 | 20 | 0.1 | 0.2 | 0.06 | $12.58^{o}$ |
| 74. | 20-0.1-0.2-0.12 | 20 | 0.1 | 0.2 | 0.12 | $8.01^{o}$ |
| 75. | 20-0.1-0.4-0.06 | 20 | 0.1 | 0.4 | 0.06 | $11.18^{o}$ |
| 76. | 20-0.1-0.4-0.12 | 20 | 0.1 | 0.4 | 0.12 | $9.37^{o}$ |
| 77. | 20-0.1-0.6-0.06 | 20 | 0.1 | 0.6 | 0.06 | $5.06^{o}$ |
| 78. | 20-0.1-0.6-0.12 | 20 | 0.1 | 0.6 | 0.12 | $3.11^{o}$ |
| 79. | 20-0.2-0.2-0.06 | 20 | 0.2 | 0.2 | 0.06 | $16.85^{o}$ |
| 80. | 20-0.2-0.2-0.12 | 20 | 0.2 | 0.2 | 0.12 | $18.65^{o}$ |
| 81. | 20-0.2-0.4-0.06 | 20 | 0.2 | 0.4 | 0.06 | $17.18^{o}$ |
| 82. | 20-0.2-0.4-0.12 | 20 | 0.2 | 0.4 | 0.12 | $16.98^{o}$ |
| 83. | 20-0.2-0.6-0.06 | 20 | 0.2 | 0.6 | 0.06 | $9.7^{o}$ |
| 84. | 20-0.2-0.6-0.12 | 20 | 0.2 | 0.6 | 0.12 | $7.05^{o}$ |
| 85. | 20-0.3-0.2-0.06 | 20 | 0.3 | 0.2 | 0.06 | Sticky |
| 86. | 20-0.3-0.2-0.12 | 20 | 0.3 | 0.2 | 0.12 | Sticky |
| 87. | 20-0.3-0.4-0.06 | 20 | 0.3 | 0.4 | 0.06 | Sticky |
| 88. | 20-0.3-0.4-0.12 | 20 | 0.3 | 0.4 | 0.12 | Sticky |
| 89. | 20-0.3-0.6-0.06 | 20 | 0.3 | 0.6 | 0.06 | Sticky |
| 90. | 20-0.3-0.6-0.12 | 20 | 0.3 | 0.6 | 0.12 | Sticky |
| 91. | 20-0.4-0.2-0.06 | 20 | 0.4 | 0.2 | 0.06 | Sticky |
| 92. | 20-0.4-0.2-0.12 | 20 | 0.4 | 0.2 | 0.12 | Sticky |
| 93. | 20-0.4-0.4-0.06 | 20 | 0.4 | 0.4 | 0.06 | Sticky |
| 94. | 20-0.4-0.4-0.12 | 20 | 0.4 | 0.4 | 0.12 | Sticky |